

Contents lists available at ScienceDirect

Advances in Colloid and Interface Science

journal homepage: www.elsevier.com/locate/cis



Historical perspective

Fundamental interfacial mechanisms underlying electrofreezing



Palash V. Acharya, Vaibhav Bahadur *

Texas Materials Institute & Department of Mechanical Engineering, The University of Texas at Austin, Austin, TX 78712, United States

ARTICLE INFO

Available online 8 December 2017

Keywords:
Electrofreezing
Electric field
Ice nucleation
Molecular dynamics simulations
Pyroelectric effect
Electrowetting

ABSTRACT

This article reviews the fundamental interfacial mechanisms underlying electrofreezing (promotion of ice nucleation via the application of an electric field). Electrofreezing has been an active research topic for many decades, with applications in food preservation, cryopreservation, cryogenics and ice formation. There is substantial literature detailing experimental and simulations-based studies, which aim to understand the complex mechanisms underlying accelerated ice nucleation in the presence of electric fields and electrical charge. This work provides a critical review of all such studies. It is noted that application-focused studies of electrofreezing are excluded from this review; such studies have been previously reviewed in literature. This review focuses only on fundamental studies, which analyze the physical mechanisms underlying electrofreezing. Topics reviewed include experimental studies on electrofreezing (DC and AC electric fields), pyroelectricity-based control of freezing, molecular dynamics simulations of electrofreezing, and thermodynamics-based explanations of electrofreezing. Overall, it is seen that electrofreezing can enable disruptive advancements in the control of liquid-to-solid phase change, and that our current understanding of the underlying mechanisms can be significantly improved through further studies of various interfacial effects coming into play.

© 2017 Elsevier B.V. All rights reserved.

Contents

1.			
2.	Role o	of applied	electric fields on electrofreezing
	2.1.	Influenc	te of DC electric fields on electrofreezing-experimental studies
		2.1.1.	1951–1980
		2.1.2.	1981–2000
		2.1.3.	2001–2017
	2.2.	Influenc	ee of AC electric fields on electrofreezing-experimental studies
3.	Influe	nce of ele	ectrical charge on freezing
	3.1.	Influenc	te of free charge in a liquid on freezing
	3.2.	Influenc	ce of surface charge on freezing
4.	Analy	sis and si	mulations of electrofreezing
	4.1.	Thermo	dynamic view of electrofreezing
	4.2.	Molecul	lar Dynamics Simulations (MDS)
		4.2.1.	Effect of an electric field on molecular structure of bulk water
		4.2.2.	Effect of charged surfaces or local electric fields on interfacial water molecules
		4.2.3.	Confinement-induced solidification
		4.2.4.	Benchmarking MDS-based studies
5.	Concl	usions an	d future outlook
Ackı	nowled	gements	
Refe	rences		

1. Introduction

The transition between water and ice is arguably the most important phase change phenomena that influences mankind. Water-ice transitions influence earth-scale events (precipitation, cloud formation,

Corresponding author.
 E-mail address: vb@austin.utexas.edu (V. Bahadur).

melting of polar icecaps) [1–6], industrial systems and processes (food preservation, aviation, shipping, infrastructure, energy efficiency etc.) [7–14] and daily life events (ice buildup, deicing roadways etc.). There are numerous studies on various aspects of water-ice transitions. While the thermodynamic freezing point of water is 0 °C, it is less well known that undisturbed water can exist as a liquid at far lower temperatures; as low as $-48\,^{\circ}\mathrm{C}$ [15], in the absence of ice nucleating agents or events. In fact, most experimental studies on ice formation rely on supercooling water (below the freezing point) to initiate ice formation. Ice nucleation is also facilitated by surfaces (heterogeneous nucleation [16]) since the energy barrier for ice nucleation is lowered [17]. Actual physical surfaces are not needed, foreign particles in water can also act as heterogeneous nucleation sites. In the complete absence of any nucleation sites, homogeneous nucleation of ice will occur, but at higher supercooling than heterogeneous nucleation.

Significant research on ice formation is motivated by anti-icing and de-icing applications. Ice buildup results in issues related to efficiency, safety and economics in sectors such as infrastructure, energy and transportation. Active (power consuming) and passive techniques for preventing ice formation, as well as deicing have received significant research attention [18–20]. One promising area, which has generated interest over the past two decades is superhydrophobicity-based icephobic surfaces [21–25]. Surface engineering and surface chemistry are powerful tools to prevent ice buildup; however further research is needed in the areas of scalable manufacturing, durability and performance degradation.

In contrast to icephobicity, this manuscript reviews studies on promoting ice nucleation via the use of electric fields. Electrofreezing has been an active research topic for many decades, with applications including food preservation, cryopreservation, cryogenics and ice formation. The food industry commonly uses methods like cryogenic freezing, air blast freezing etc. to accelerate and control freezing. Product quality depends on the freezing rate, which directly influences the spatial and temporal dynamics of ice growth. For instance, an unregulated intracellular matrix ice growth is undesirable in food and bioprocessing industries due to resulting damage to the cellular tissue [7–11]. On the other hand, industries such as freeze-drying and freeze concentration prefer relatively larger ice crystals in drying-based lyophilization processes [12,26]. The ability to control the rate of ice formation and the structure of ice via control of freezing parameters is critical in such applications.

While current studies on electrofreezing are primarily motivated by applications related to food preservation, early studies were conducted with the objective of understanding the role of electrical phenomena on ice formation in tropospheric clouds. Ice formation in clouds can be attributed to the presence of aerosol particles which act as heterogeneous nucleation sites. Local electric fields, charged aerosol particles or by-products of atmospheric ionization resulting from thunderstorms have also been studied for their freezing-inducing tendencies [27–29]. Atmospheric ice formation is the topic of several extensive reviews [27–35], and is not discussed in this work.

This work reviews the fundamental mechanisms underlying ice nucleation under the influence of electric fields and electrical charges. Experimental and simulation-based studies from 1861 to date are reviewed. The mechanisms and theories proposed to explain various aspects of electrofreezing are summarized and analyzed. The primary objective of this critical review is to analyze and summarize all such studies and highlight the similarities and discrepancies between various perspectives. It is noted that application-relevant studies of electrofreezing which involve protein crystallization, food preservation, cryofreezing, atmospheric icing and others are excluded from this review; such studies have been reviewed in recent literature [36–49]. This review focuses only on studies, which analyze the physical mechanisms underlying the influence of electric fields and electrical charge on freezing, without any focus on specific applications.

This article commences with a review of experimental studies on electric field-based control and enhancement of freezing (Section 2).

Section 3 reviews experimental studies on the role of electrical charges on freezing. Section 4 reviews theoretical and modeling-based studies on electrofreezing. Section 4 is divided into two subsections, which review thermodynamics-based explanations of electrofreezing and molecular dynamics simulations-based studies on various aspects of electrofreezing.

2. Role of applied electric fields on electrofreezing

This section reviews experimental studies on the influence of externally applied electric fields on ice nucleation. The influence of DC and AC electric fields is separately discussed. It is noted that most experimental studies follow one of the two experimental procedures below:

- Supercooling water under the influence of an electric field at a fixed cooling rate, and measuring the ice nucleation temperature. The strength of the electrofreezing effect is quantified via the observation of higher nucleation temperatures.
- Supercooling water to a predetermined temperature, followed by turning on the electric field. The measurement of interest is the induction time (time from the application of the electric field to the onset of nucleation), with lower induction times indicating more effective electrofreezing.

2.1. Influence of DC electric fields on electrofreezing-experimental studies

The majority of experimental studies on electrofreezing have utilized DC fields. The first-ever demonstration of electrofreezing was by Dufour [50] in 1861, wherein electric fields were observed to initiate freezing in supercooled water droplets. Following this study, there was a century-long hiatus on experimental studies. Subsequent studies can be conveniently summarized and analyzed by grouping them into three time periods as detailed ahead.

2.1.1. 1951-1980

This period includes experimental studies on the role of electrical phenomena in triggering ice nucleation in cirrus clouds [30]. Some studies also analyzed ice formation in the vicinity of high voltage conductors [51]. These studies led to the emergence of multiple theories and mechanisms underlying electrofreezing, many of which were validated in subsequent experimental studies and molecular dynamics simulations. Key studies and the proposed mechanisms underlying electrofreezing are reviewed ahead.

2.1.1.1. Role of surfaces and the three-phase contact line. Schaefer (in 1953) observed the freezing of supercooled water droplets resting on a plastic surface subjected to electric discharges from a Tesla coil [52]. No freezing was noticed when supercooled water droplets floating in air in a cold chamber were subjected to the same discharge. This suggested the combined interplay of an electric field and a surface on electrofreezing.

In early studies, freezing water droplets were exposed to an electrical discharge since the electric fields exceeded the threshold for electrical breakdown. In 1963, Pruppacher [53] designed experiments wherein water droplets were subject to electric fields of up to 6×10^6 V/m without the surrounding medium undergoing breakdown. Results indicated that electrofreezing was not due to particulate matter produced in corona discharges, or the polarization of water. Ice nucleation was always initiated at a moving three-phase contact line on a surface in the presence of an electric field; this was observed for DC and AC electric fields. It was proposed that the movement of the three-phase line results in charge transfer from the surface to the bulk of the liquid, resulting from the movement of the electrical double layer. These incoming charges stabilize the accumulating water clusters in the bulk of the supercooled droplet, thereby producing an ice nucleus which initiates freezing upon reaching a critical size.

2.1.1.2. Liquid filament formation-induced nucleation. Loeb [54] proposed that the water surface gets drawn out into tiny filaments when the force resulting from the applied electric field overcomes the surface tension. This results in the formation of minute crystallites at the tip of these filaments, which at length scales <1 μ m diameter act as nucleating agents [54,55]. Based on Prupaccher's results [53], Loeb proposed the following necessary prerequisites for nucleation:

- Liquid surface needs to be drawn out into tiny filaments of a dimension comparable to the size of a crystallite.
- A solid near the nucleation site is essential to dissipate the latent heat of crystallization (this explains the non-freezing of droplets when suspended in a chamber, as reported by Schaefer [52]).
- Space is required near the contact line for water to expand on freezing.

Further studies [56–58] showed that electrofreezing was triggered by the disruption of the droplet-air interface instead of the movement of a three-phase line. Such disruptions can be triggered electrically or mechanically. Electric-field-induced surface disruption led to longer filaments when compared to mechanical disruption, thereby enhancing nucleation to a larger extent. This is evident from the work of Abbas and Latham [56], wherein a greater fraction of droplets froze (Fig. 1) when disrupted by an electric field, as against mechanical disruption from a penetrating insulating fiber.

2.1.1.3. Acoustic shock due to cavitation of dissolved gases in water. Smith et al. [59] studied the freezing of supercooled water droplets (radius: 2 mm) at temperatures ranging from 0 to $-12\,^{\circ}$ C, falling vertically through electric fields. It was reported that the fraction of frozen droplets increased steadily from 0 at $-5\,^{\circ}$ C to 0.6 at $-10\,^{\circ}$ C only in cases where the electric field was turned on. Notably, the results are close to the findings of Abbas and Latham [56] (Fig. 1). No enhancement in freezing fraction was observed in the absence of an electric field. Furthermore, the probability of freezing was unaffected by the passage of a spark through the medium. It was suggested that the collapse of cavities (due to cavitation of dissolved gases in the liquid) resulting from vibrations of the droplet surface increases the local pressure of the surrounding fluid. This elevates the equilibrium freezing temperature of the surrounding fluid, thereby inducing nucleation at a lower degree of supercooling.

2.1.1.4. Presence of an adsorbed layer on the solid surface. In 1973, Pruppacher [60] discussed a new mechanism to explain electrofreezing, which used the concept of adsorbed layers, proposed by Evans [61]. According to Evans [61], nucleation in the bulk of a liquid proceeds from a thin layer of interfacial water firmly adsorbed on the surface, as

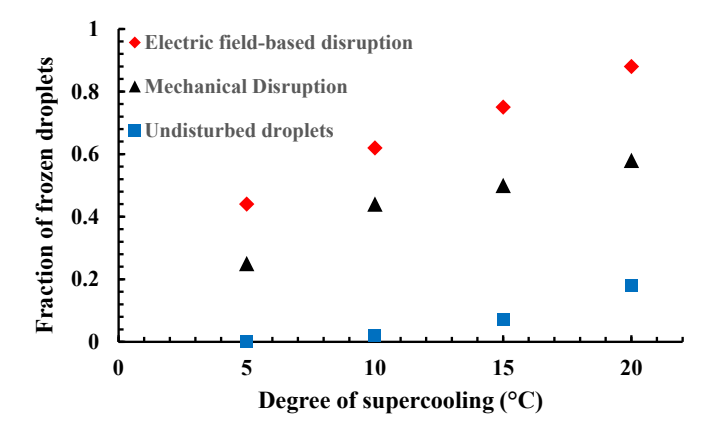


Fig. 1. Fraction of water droplets (radius: 1 mm) frozen under different conditions and temperatures. Electric fields enable more effective freezing as compared to mechanical disturbances. This plot is based on data reported in Reference 56. The applied electric field ranged from 0 to 15×10^5 V/m.

against the conventional notion that freezing initiates directly on the surface. The molecules in a freshly adsorbed water layer can be easily reoriented and ice nucleation is quicker when compared with a firmly adsorbed layer. For firmly adsorbed water layers, which are oriented by the surface, a higher degree of supercooling is required to enable a 2-D transformation of this layer to a structure similar to that of ice. However, when this layer freshly wets the surface in a transient fashion (as in the case of a moving contact line as observed by Pruppacher [53]), or is loosely bonded to the surface, it is energetically favorable to bring about the same transformation at lower supercooling by applying an electric field. This theory of disordered layers has been investigated via molecular dynamics simulations, which confirm the presence of such adsorbed layers and their role in ice nucleation [147,149,162,163].

2.1.1.5. Local dipole field interaction. In 1951, Rau [62] studied electrofreezing of water droplets on a chromium surface (negative electrode). Droplets were seen to freeze following an electric spark produced by a positive point electrode on top of the droplet. Similarly, freezing was initiated by a spherical electrode covered with a dielectric without the initiation of a spark at temperatures as high as – 4 °C for electric fields ranging from 2 to 6 \times 10⁵ V/m. It was suggested that the electric field rearranges water clusters due to polarization, thereby creating a structure more favorable for ice nucleation.

A similar theory was proposed by Salt [63] to explain the freezing of supercooled water droplets under an AC field. Pruppacher [53] refuted this theory based on observations that electric fields as high as 3×10^6 V/m were insufficient to induce freezing in a water column. Gabarashvili & Gliki [64] noted that the electric field experienced by a layer of water molecules would be enhanced on the surfaces of charged particles, due to projections on surfaces. The resulting polarization of water molecules adjacent to the surface stabilizes subsequent layers thereby assisting freezing. The electric field near the surface projections of naphthalene particles charged to 3000 V was estimated to reach 7.2×10^8 V/m [64]. This theory of polarization of local water molecules (adjacent to charged surfaces) has also been studied via experiments and simulations in recent years.

2.1.1.6. Studies which did not detect electrofreezing. It is noted that not all early studies on electrofreezing yielded positive results. Dawson and Cardell [65] (1973) measured the freezing probability of droplets supercooled to temperatures ranging from -8 to $-15\,^{\circ}\text{C}$, under the influence of electric fields up to $10^6\,\text{V/m}$. No electrofreezing was detected even under three favorable circumstances: high electric fields that led to droplet instability, collision of charged and uncharged droplets in the electric field, and the presence of corona discharge. Similar results were reported by Doolittle and Vali [66] (1974) wherein it was observed that electric fields up to $6\times10^5\,\text{V/m}$ had no intrinsic effect on the heterogeneous freezing of water droplets containing leaf derived nuclei and silver iodide based colloids.

2.1.2. 1981-2000

There are relatively fewer experimental studies in the last two decades of the twentieth century; however, some studies in this period are the basis for significant later progress. Shichiri and Nagata [67] studied the influence of electric current and electrode material on the nucleation of ice crystals. They observed that an electric current elevated the nucleation temperature. Furthermore, nucleation initiated at the cathode and anode for electrode materials having low and high ionization tendencies, respectively. Another mechanism associated with the flow of electric current is bubble generation due to electrolysis at the electrodes. It was inferred by Sivanesan & Gobinathan [68] that electrolytic bubble generation and its subsequent collapse, along with a favorable orientation of the water layer adjacent to the electrodes could be possible mechanisms underlying electrofreezing. Shichiri &

Araki [69] proposed that the attraction of the dipoles (in water) to surface charge leads to supersaturation of water molecules in a bubble near the electrode surface. This results in heterogeneous nucleation of an ice crystal in the vapor phase. This crystal deposits on the electrode surface when the bubble departs and acts as the seed for further nucleation/growth.

The structural similarity of the substrate with that of ice has been considered an important criteria for a solid to be a good ice-nucleant [1]. Gavish et al. [70] studied freezing on hydrophobic surfaces of polar and nonpolar amino acid crystals with a crystalline structure different from that of ice. Crystals which exhibited a polar axis demonstrated freezing temperatures higher by 3–5 °C when compared to their non-polar counterparts. It was initially hypothesized [70] that concentrated electric fields within the cracks in the crystals, with a magnitude large enough to induce a phase transformation of the interfacial water molecules were responsible for promoting nucleation. However, it was later shown through similar experiments that the pyroelectric charge is responsible for electrofreezing instead of the hypothesis proposed by Gavish et al. [70]. Pyroelectric effect-based electrofreezing is discussed in detail in Section 3.2.

Braslavsky and Lipson [71] (1997) reported an electrofreezing temperature of $-0.1\,^{\circ}\text{C}$, which is the highest recorded freezing temperature under electric fields. This was however accompanied by a very long crystal propagation time (8 h) and was dependent on the long-term temperature stability of the surrounding growth medium. The experiment involved locally supercooling part of the liquid with a Peltier cooling system followed by the passage of high voltage pulses (10 μ s pulse of 10,000 V) through the liquid.

2.1.3, 2001-2017

The period since 2000 has produced several significant studies, which clearly highlight the varied, multiphysics and complex mechanisms underlying electrofreezing. Key studies and mechanisms discovered during this period are summarized ahead.

2.1.3.1. Influence of electrode material and geometry. Hozumi et al. [72] and Hozumi et al. [73], studied the influence of electrode material and geometry on electrofreezing. Nucleation was observed to initiate from the anode when the electrode metal had a high ionization tendency. It was hypothesized that polynuclear coordination compound-based complexes were being formed; the similarity of the structure of these complexes to the hexagonal structure of ice was hypothesized as being responsible for electrofreezing. This study established the following order of metals, arranged in descending order of their ability to electrofreeze water: Al, Cu > Ag > Au > Pt > C. Similar results were earlier reported by Shichiri and Nagata [67] who correlated the propensity to electrofreeze with the ionization potential. Having explored the influence of material properties, Hozumi et al. [73] studied the effect of electrode geometry on electrofreezing, using various combinations of flat and sharp electrode geometries for the cathode and anode (Fig. 2). The experimentally determined propensity to electrofreeze, in



decreasing order, was [73]:

where a & c denote the anode and cathode respectively. The flat geometry configuration of anode houses a higher surface density of ions due to the presence of numerous micro-convex surfaces, as compared to a sharp geometry. This results in a larger density of interfacial coordination compounds, which translates to accelerated electrofreezing.

2.1.3.2. Confinement-induced electrofreezing. Choi et al. [74] observed electric field-dependent freezing of water confined between two electrodes with molecular-level spacing at room temperature. Fig. 3a shows a schematic of the experimental setup. The concept underlying confinement-induced freezing is the reduction in translational entropy of water molecules confined in gaps (a few molecular layers thick), which induces solidification. Electric fields enhance this effect by inducing a perturbation in the water network by exerting a torque on the molecules to restructure them into an ordered hydrogen-bonding network. It was reported [74] that the critical gap for inducing freezing was approximately 14 Angstrom, which is the thickness of 3–4 molecular layers of water. The electric field required ranged from (2–8) \times $10^6\,\mathrm{V/m}$. It is noted that this field is much less than molecular dynamics simulations-based predictions of electric fields required to induce dipole polarization in water (>10^9\,\mathrm{V/m}).

It is noted that very high electric fields ($\sim 10^9$ V/m) are challenging to apply due to limitations in experimental setups and the dielectric breakdown strength of water, which is (O)10⁷ V/m and (O)10⁸ V/m for millimeter and micrometer scale volumes of water, respectively [75,76]. Furthermore, the effective electric field in the inside (bulk) of a spherical droplet (E_{in}) is less than the electric field outside the droplet (E_{out}), when the droplet is not in direct contact with electrodes. The relation is [77]:

$$E_{in} = \left(\frac{3\varepsilon_{out}}{\varepsilon_{water} + 2\varepsilon_{out}}\right) E_{out} \tag{1}$$

where, $\varepsilon_{out} \& \varepsilon_{water}$ denote the dielectric constants of the surrounding medium and water, respectively. This relation suggests that an applied electric field of (O)10⁹ V/m would effectively only produce an internal field of (O)10⁷ V/m, thereby attenuating the applied field by at least two orders of magnitude inside the droplet.

2.1.3.3. Influence of an electric field on homogeneous nucleation. Stan et al. [78] quantified the influence of an electric field on homogeneous nucleation; a schematic of the experimental setup is shown in Fig. 3b. Discrete water droplets traveled in a flow cell with a transverse electric field, where they cooled until they froze. Based on the experimental results, and thermodynamic analysis, it was estimated that the minimum electric field to produce any perceivable change in nucleation is 1.8×10^7 V/m. Furthermore, it was reported that electric fields of O(10^8) V/m enhance the nucleation rate due to the formation of ferroelectric ice (ice XI).



Fig. 2. Electrolytic bubble formation at cathode [73] (a) A sharp cathode produces a larger hydrogen bubble, which interferes with coordination compound formation at the anode (b) A flat cathode, on the other hand, produces a large number of smaller bubbles which do not affect reactions occurring at the anode. This explains the observed higher electrofreezing tendency with flat cathodes as compared to a sharp cathode. Figs. 2 reprinted with permission from Reference [73].

Copyright: 2005 by Elsevier.

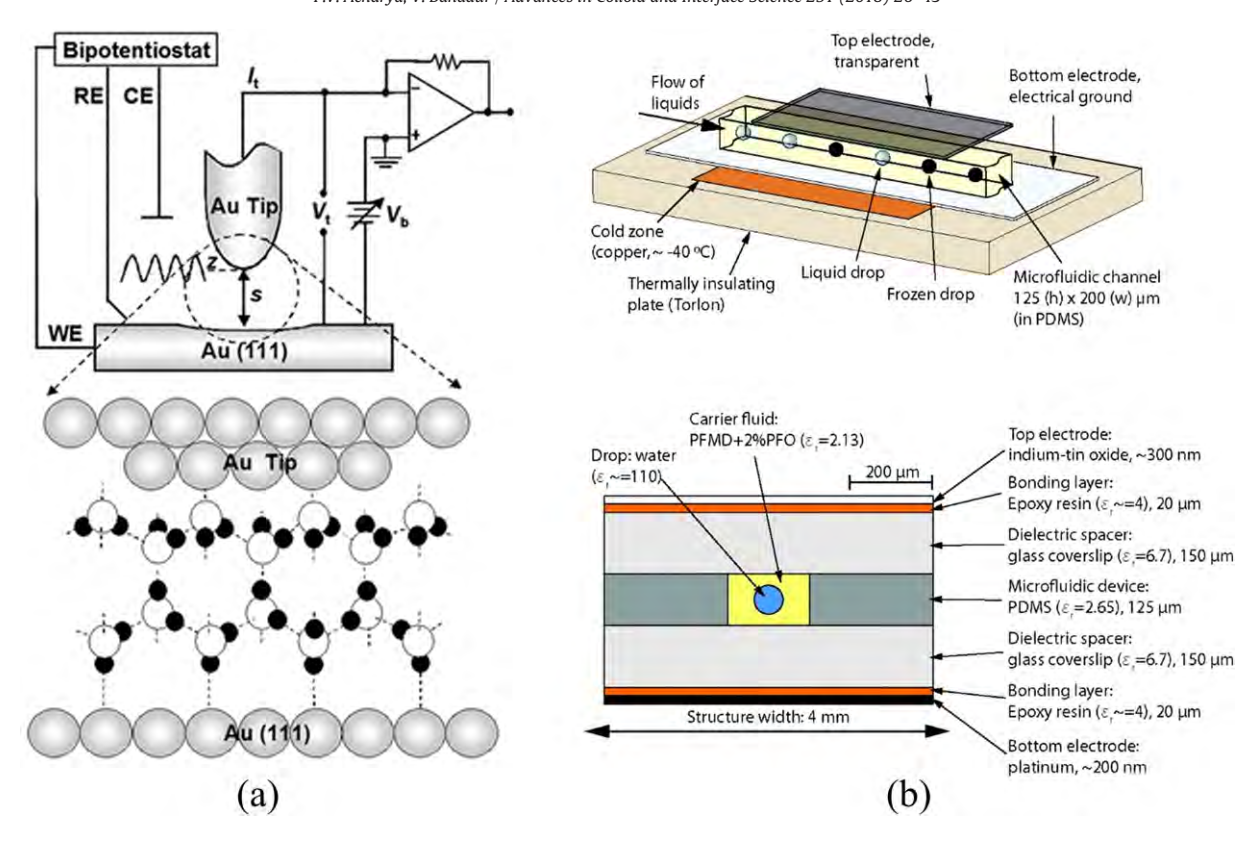


Fig. 3. (a) Schematic of experimental setup to observe confinement-induced freezing under an electric field [74]. Water is present in the gap between the gold tip and the negatively biased gold (111) surface. A piezo driver of known sensitivity controls gap spacing. The black and white spheres represent hydrogen and oxygen molecules in a bilayer of water molecules respectively. (b) Schematic of experimental setup to study the role of an electric field on homogeneous nucleation [78]. Droplets travel through a microfluidic channel cooled to -40° C under a transverse electric field. Fig. 3(a) reprinted with permission from Reference [74]. *Copyright: 2005 American Physical Society.* Fig. 3(b) reprinted with permission from Reference [78]. *Copyright: 2011 American Chemical Society.*

2.1.3.4. Electrofreezing in electrowetting on dielectric configurations. Recent studies have analyzed electrofreezing via experiments using an experimental configuration typically used for studies on electrowetting. Electrowetting [79] is a well-known microfluidic technique to change the wettability of droplets via an applied electric field. This electric field exists in a dielectric layer beneath a static droplet (Fig. 4b). The droplet has higher electrical conductivity than the dielectric and can be considered equipotential. Nakajima et al. [80] (2007) investigated the effect of 3-phase contact line movement (using electrowettingbased actuation) on freezing of supercooled water droplets on a hydrophobic surface. It was observed that contact line motion enhances electrofreezing; these results corroborate the observations of Pruppacher [53], almost five decades ago. Daniel et al. [81] studied the influence of charge-induced filamentation on freezing of supercooled water droplets; this filamentation is the result of a Coulombic instability when the surface charge exceeds the Rayleigh limit. No perceivable influence of filamentation in inducing freezing was observed.

Yang et al. [82] (2015) studied the dynamics of ice-nucleation in supercooled water droplets in an electrowetting setup using electric fields of (O) 10⁶ V/m. High-speed visualization (Fig. 4a) showed that nucleation initiates at the three-phase line and that this phenomenon is polarity-independent. Importantly, it was seen that contact line motion due to the electric field was essential for nucleation. Contact line motion in the absence of an electric field, as well as the application of an electric field without contact line motion, failed to initiate nucleation.

Carpenter and Bahadur [83] used an electrowetting setup to isolate the influence of electric field and electric current on electrofreezing (Fig. 4b). The maximum electric field used in this study was 80 \times 10^6 V/m, which is $13\times$ higher than the previously highest field (6 \times 10^6 V/m) utilized. Electric field (in the absence of current flow) elevated freezing temperatures by >15 °C, with the polarity-

independent electrofreezing effect saturating at high electric fields (> 20×10^6 V/m). Additionally, by intentionally introducing pinholes in the electrowetting dielectric layer, passages for current flow were established and electrofreezing experiments were conducted in the presence of electric current. Current flow enhanced the electrofreezing effect, over that obtained by electric field alone (Fig. 4b). Similar results were also obtained by Shichiri and Nagata [67].

2.1.3.5. Electrofreezing of hydrates. Carpenter and Bahadur [84] and Shahriari et al. [85] showed that electrofreezing can significantly accelerate the nucleation of clathrate hydrates. Clathrate hydrates are waterbased crystalline solids consisting of a guest molecule (methane, carbon dioxide, tetrahydrofuran, cyclopentane etc.) in a lattice of water molecules, and typically form at temperatures around 0 °C. A significant challenge underlying the synthesis of hydrates is the long induction (wait) time before hydrates form. This can range from hours to days and is a big hindrance to the realization of applications which require synthesis of hydrates. It was shown (Fig. 5a) that electric fields reduce the induction time for tetrahydrofuran hydrate formation by $> 100 \times$. The use of aluminum-foam based electrode as the anode resulted in a $150 \times$ reduction in induction time as compared to bare metal electrodes; nucleation was observed in 10's of seconds (almost instantaneous nucleation). Electrofreezing was observed to strongly depend on electrode polarity [85]. Two distinct mechanisms (electrolytic bubble generation at cathode & formation of aluminum-based coordination compound complexes at anode) were experimentally uncovered (Fig. 5b), which explains polarity-dependent electrofreezing with electrode materials having high ionization tendencies.

2.1.3.6. How strong is the electrofreezing effect?. Table 1 summarizes experimental measurements of the nucleation temperature and the

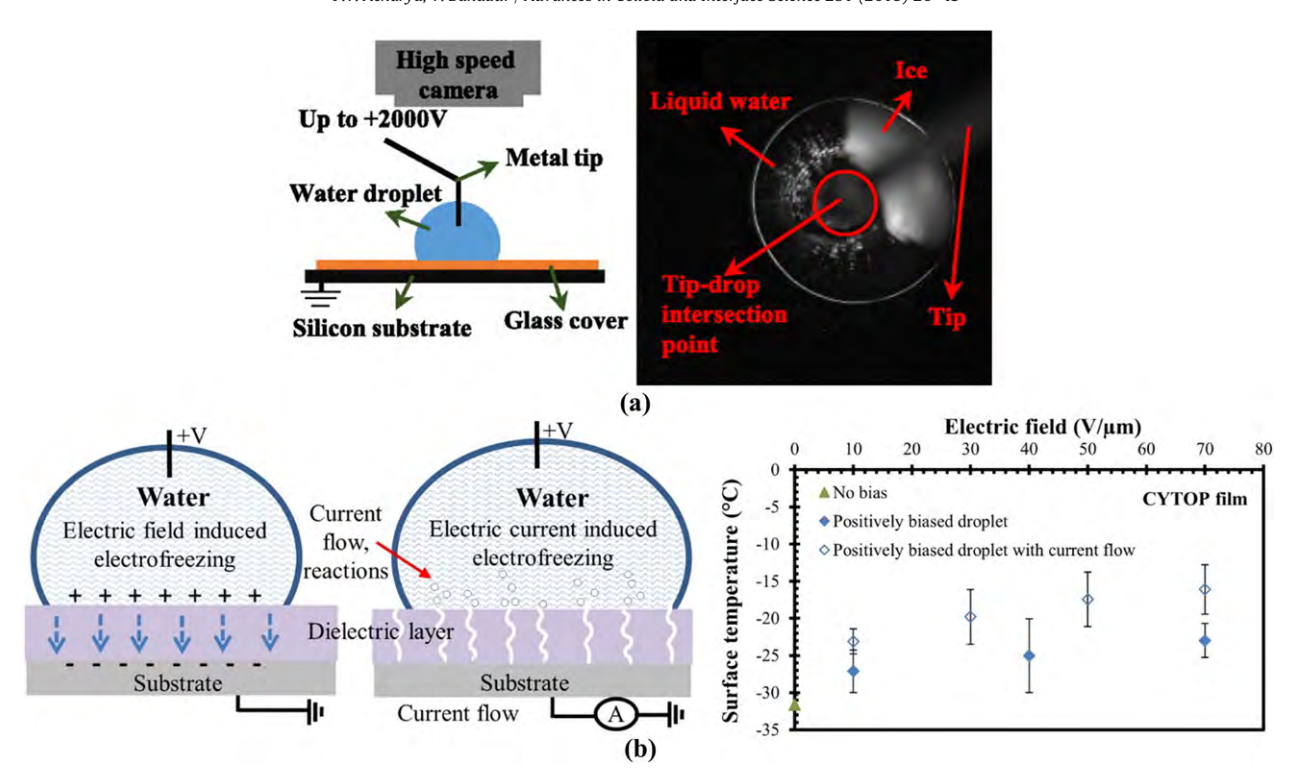


Fig. 4. Electrowetting-based experimental setups used for studies on electrofreezing (a) Top view of nucleation and phase front propagation inside a droplet [82]. Electrofreezing commences at the three-phase line, with multiple nucleation points at higher voltages. (b) Experiments to isolate the influence of electric field and current flow on electrofreezing [83]. Results indicate that both phenomena influence electrofreezing. Fig. 4(a) reprinted with permission from Reference [82]. *Copyright: 2015 AIP Publishing LLC.* Fig. 4(b) reprinted with permission from Reference [83]. *Copyright: 2015 American Chemical Society.*

phase transformation time (time required to convert the entire mass of water to ice) from various experimental studies. It is seen that while the experiments differ in methodology, volume of water used and the method of applying the electric field, most studies show an increase in

the nucleation temperature (reduced supercooling requirement) when compared to the no electric field case.

The influence of an electric field on the freezing temperature can be quantified by two metrics: the nucleation temperature, and the

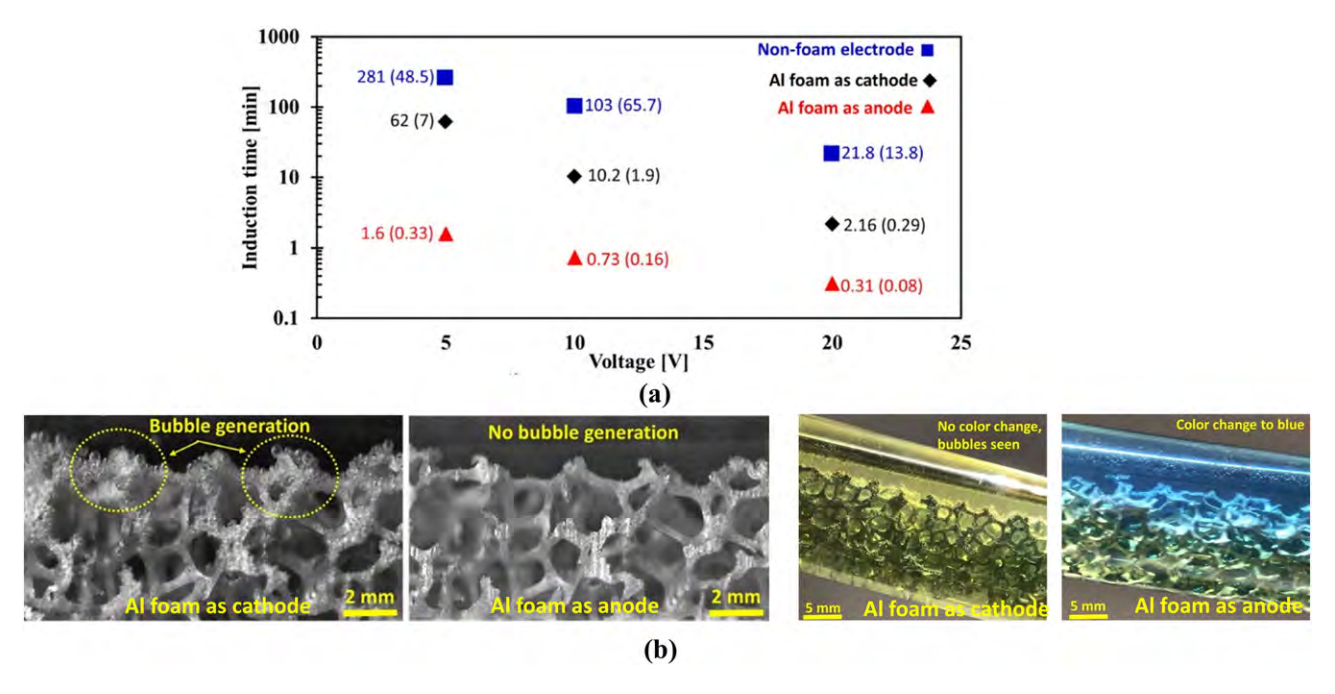


Fig. 5. (a) Voltage-dependent induction times for nucleation of tetrahydrofuran hydrates with aluminum foam as the electrofreezing electrode. The numbers in parenthesis indicate the induction time and standard deviation, respectively. Electrofreezing clearly accelerates hydrate nucleation, with the electrofreezing effect strongly dependent on the polarity of the aluminum foam [85]. (b) Two polarity-dependent mechanisms underlying electrofreezing were uncovered. Aluminum foam as the cathode leads to electrolytic bubble generation (left two images of 5b); bubbles provide the activation energy to initiate nucleation. Aluminum foam, when used as anode leads to the formation of aluminum-based coordination compounds, which assist nucleation (these are detected via a colorimetric reaction, as seen in the two right images of 5b) [85]. Figs. 5 (a) & (b) reprinted with permission from Reference [85]. Copyright: 2017 American Chemical Society.

Table 1Summary of experimental studies on electrofreezing.

Reference and year	Electrode material/configuration	Volume	Electric field $(\times 10^5 \text{ V/m})$	Mean temperature of nucleation (°C)	Mean phase transformation time (s)	Significant findings
Doolittle and Vali (1975) [88]	Wire grid based top electrode. Silicone varnished bottom electrode.	10 μl water droplets containing organic nuclei or AgI colloids	6	-	-	Electric fields up to 6×10^5 V/m do not affect heterogeneous nucleation.
Sivanesan and Gobinathan (1991) [68]	Copper electrodes immersed in a tube containing liquid	50 ml	0.1	-4 °C (pure water) -1.0 °C (50:50 Agl: CuBr mole %) -1.1 °C (90:10 Agl:CuBr mole %)	-	Electric fields of magnitude (O) 10 ⁴ V/m reduce supercooling requirement in presence of Agl-CuBr nucleants
Wei et al. (2008) [86]	Parallel plate copper electrode (spacing 20 mm); liquid not in contact with electrodes	1 ml (water)	No field 0.01 0.05 0.5 1	$\begin{array}{c} -7.27 \pm 0.56 \\ -7.31 \pm 0.44 \\ -7.15 \pm 0.63 \\ -6.32 \pm 0.37 \\ -5.68 \pm 0.36 \end{array}$	714 ± 64 720 ± 61 718 ± 56 803 ± 17 829 ± 36	Phase transformation time is inversely proportional to nucleation temperature.
Orlowska et al. (2009) [87]	Parallel plate aluminum electrodes (spacing 2.2 mm); liquid not in contact with electrodes	1.6 ml (water)	No field 10 25 50 60	-12.28 ± 2.19 -9.16 ± 0.72 -7.36 ± 1.113 -6.64 ± 0.95 -5.90 ± 1.39	303 ± 43 350 ± 17 371 ± 21 403 ± 32 393 ± 24	
Yahong et al. (2010) [89]	Gold plated copper electrodes	0.5 ml of 0.9 wt% NaCl solution	0 0.005 0.01	-5.9 -6.9 -7.4	_	Supercooling temperature reduces with electric field
Jankowski and McCluskey (2010) [90]	Cylindrical silver wires used. Separation between pointed tips: 350 µm	5 g of melted erythritol	-	108–112 (6–10° supercooling with electric field)	-	Electric current reduces required supercooling magnitude range from 9-51 °C to 6-10 °C
Stan et al. (2010) [78]	Top electrode: Indium-tin oxide covered with a dielectric spacer Bottom electrode: platinum covered with dielectric spacer	Water droplets (diameter 100 μm)	$1.6 \pm 0.4 (AC)$	-	-	AC electric fields up to $(1.6 \pm 0.4) \times 10^5$ modified homogeneous nucleation rate by $< 1.5 \times$
Yang et al. (2015) [82]	Bottom substrate covered by a dielectric layer, with wire at top	20 µl (water)	27 36 45	-23.7 ± 0.7 -23.3 ± 2.4 -23.2 ± 1.6	-	Electric fields <5 V/µm have small influence on nucleation.
Carpenter and Bahadur (2015) [83]	Droplet resting on dielectric layer. Thin wire biases droplet.	5 μl (water)	No field 100 200 400 800	-30 -20 -19 -18 -17	-	 Electric fields enable electrofreezing in absence of current flow. Current flow enhances electrofreezing effect.
	Droplet resting on dielectric layer (with pinholes to allow current flow). Thin wire biases droplet.		No field 100 300 500 700	-32 -23 -20 -17 -16		
Zhang et al. (2016) [91]	Outer electrode: cylindrical shell Inner electrode: cylinder with upper surface covered with stearic acid (SA) or polyethylene (PE)	Water droplets (0.5 µl)	$0\\4.3 \pm 0.1\\0\\4.3 \pm 0.1$	- 17.75 (SA) - 16.65 (SA) - 18.75 (PE) - 18.15 (PE) - 18.05 (PE)	-	 Minimum electric field to promote nucleation is 10⁵ V/m. Increased nucleation rate ascribed to electrical double layer at waterdielectric interface. Droplet deformation has no effect on nucleation promotion

reduction in the supercooling requirements as compared to the no electric field case. Fig. 6 compiles the results of seven similar studies and shows that the required supercooling decreases with increasing electric fields. The highest electrofreezing temperature was recorded as $-0.1\,^{\circ}\text{C}$ by Braslavsky and Lipson [71]. The maximum reduction in supercooling under the influence of an electric field was 16 °C for an electric field of 80×10^6 V/m by Carpenter and Bahadur [83]. It is important to note that supercooling has been necessary in all studies other than the work of Choi et al. [74], wherein electric fields were observed to initiate freezing in water layers under confinement at room temperature.

Electrofreezing also affects the phase transformation time, which depends on the available paths to remove the heat generated during ice nucleation. As observed by multiple researchers, the onset of ice nucleation is accompanied by a sharp temperature rise to 0 °C (recalescence or Stage I freezing) as the liquid mass rearranges itself to 'freeze'. The rate of propagation of the freeze front depends on heat transfer pathways. The results of Wei et al. [86] and Orlowska et al. [87] in Table 1 show that the phase transformation time increases with the electric field. This is because of electrofreezing-induced higher nucleation temperatures, which lead to a smaller temperature difference from the freezing temperature of 0 °C. Since this temperature difference drives heat transfer, electrofreezing increases the phase transformation time, as compared to the no electric field case. Wei et al. [86] observed that the continued application of an electric field post-nucleation had no effect on the phase transformation time.

In contrast to most of the studies discussed, Wilson et al. [92] suggested that the increase in the freezing temperature due to an electric field can be attributed simply to the stochastic nature of nucleation and that previous studies did not uncover this due to a limited number of experimental runs. To demonstrate this claim, Wilson et al. conducted 300 nucleation experiments (first 170 experiments conducted in the presence of an electric field and the remaining 130 experiments with the electric field turned off); it was reported that the average nucleation temperature remained unchanged after the 170th experiment. However, most studies contradict these observations and report a statistically significant influence of an electric field on nucleation.

It is important to note that several mechanisms underlying electrofreezing were proposed during the period 1951–1980. Although some mechanisms were experimentally validated, there remain unresolved questions on the relative importance of these mechanisms. Post 1980, most experimental studies have focused on quantifying the benefits/impact of electrofreezing, and not on the underlying mechanisms. This is one reason why the studies pre-and post-1980 can seem disconnected. Overall, well-planned experimental studies are needed to clearly quantify the relative influence of various contributing mechanisms.

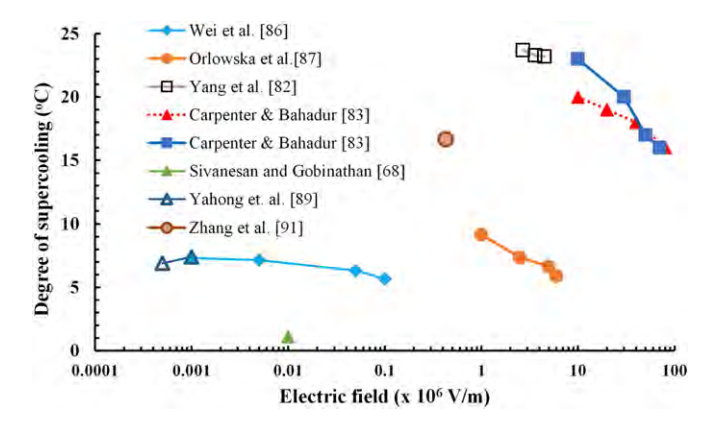


Fig. 6. Compilation of experimental results [86,87,82,83,68,102,91] on the influence of an electric field on the freezing of supercooled water. Discrepancies in the magnitude of the electric field required to induce freezing are attributed to variations in the experimental setup and procedures across these studies.

We end this section by discussing the relevance of the abovedescribed studies. Parameters like the nucleation temperature, cooling rate and phase transformation time determine the crystal growth and the resulting structure of ice. Such parameters influence processes in the food preservation and cryopreservation industries. As an illustration, a slower cooling rate or a lower degree of supercooling results in large ice crystals [93-95] which can cause cryoinjury to food tissues during intracellular freezing. However, larger crystals will result in larger pore spaces which will favorably reduce the resistance to solidvapor propagation front during lyophilization [26]. On the other hand, a faster cooling rate, the application of AC electric fields or the use of pressure shift freezing results in higher supercooling requirements [40]. This leads to smaller grain sizes with a larger number of ice crystals [36,96–98], which is preferred for meat preservation. Also, the overall freezing time decreases with increased supercooling. These aspects of freezing have been researched in studies which exclusively focus on the role of electric fields on ice crystal growth. Such studies have been reviewed [36–49] for their applications in freeze drying, protein crystallization and cryopreservation. Since the scope of the present review is limited to studies on the fundamental mechanisms underlying electrofreezing, such studies are not reviewed presently.

2.2. Influence of AC electric fields on electrofreezing-experimental studies

There are fewer studies on electrofreezing using AC electric fields. Salt [63] (1961) conducted the first such experiments with 60 Hz AC fields. Application of 1.5×10^6 V/m electric fields elevated the nucleation temperature of water from $-10\,^\circ\text{C}$ to $-2\,^\circ\text{C}$. More recent studies suggest that the use of AC electric fields can retard nucleation and increase the required supercooling. This was discussed in a patent on a non-freezing refrigerator filed by Kim [99]. Vibrations in the dipoles of water molecules, induced by AC electric fields can retract molecules from their equilibrium position as against DC electric fields which tend to structurally align the molecular network via dipole-field interaction. This suggests that AC fields will suppress cooling or effectively increase the supercooling requirement for nucleation.

This increase in the supercooling requirement and the slowdown in ice formation kinetics due to AC electric fields have been confirmed in more experimental studies [36]. Shichiri and Araki [69] reported that the AC electric fields had minimal or no effect on the nucleation temperature. Stan et al. [78] observed that AC electric fields of up to 1.6×10^5 V/m and frequencies from 3 to 100 kHz affected the homogeneous nucleation rate of supercooled water droplets by less than a factor of 1.5. Sun et al. [100] showed that the influence of an AC field on ice formation is strongly dependent on the AC frequency. It was observed that ice crystal size and freezing time of a 0.9% K₂MnO₄ solution exhibited an inverse dependence on the AC frequency, with a minimum at 50 kHz followed by an increasing trend. Wei et al. [101] observed that a 500 kHz frequency maximized the fraction of salty ice and suppressed the formation of pure ice while freezing a 0.9% NaCl solution. A micro electrofreezing chip was designed by Ma et al. [102] to obtain the optimal parameters for electrofreezing under an AC field. Ma et al. [103] further studied the effect of AC electric fields (up to $1 \times 10^5 \text{ V/m}$) with frequencies ranging from 10⁵ to 10⁷ Hz, on the freezing of a 0.9 wt% NaCl aqueous solution. It was observed that the grain size and the crystallization fraction of the resulting ice grains decrease with increasing electric field. However, these parameters show a different trend when the AC frequency is varied, with the existence of a minima (Fig. 7).

3. Influence of electrical charge on freezing

While the previous section analyzed the influence of applied electric fields on ice nucleation, there is a separate (and smaller) set of studies on the role of electrical charge on freezing (without any externally applied field). It is noted that applied fields, in turn, induce interfacial

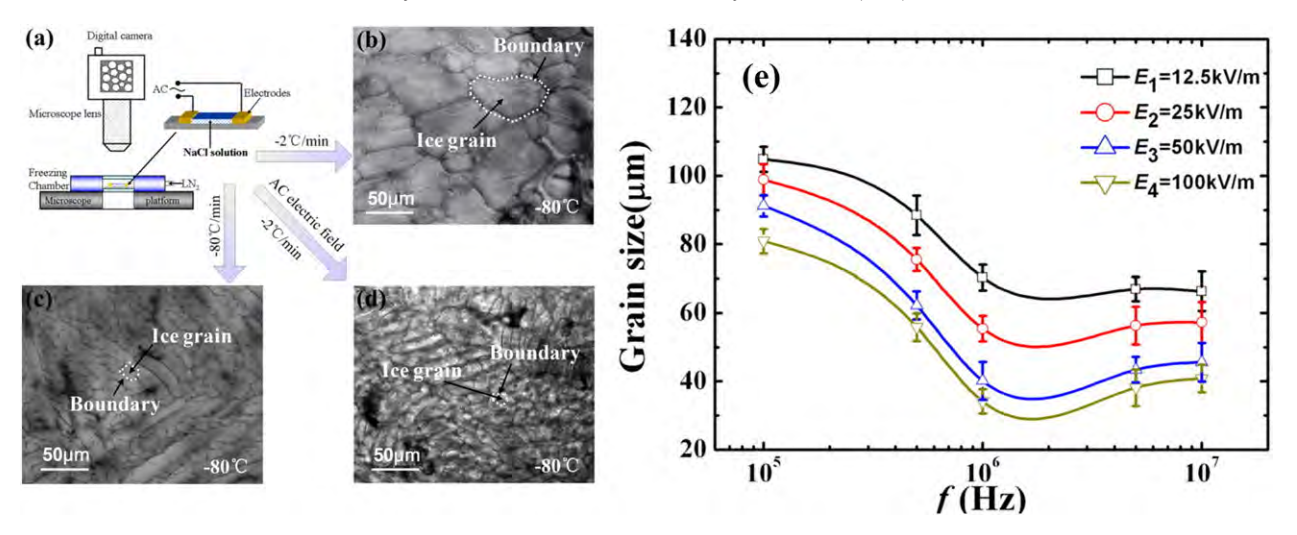


Fig. 7. (a) Schematic of the experimental study of Ma et al. [103] (b), (c) & (d) are optical images of ice formed from a freezing NaCl solution. (c) A fast cooling rate $(-80 \, ^{\circ}\text{C/min})$ results in the formation of fine crystals (average size ~40 μ m) and a higher crystallization fraction when compared to (b) ice formation under slower cooling $(-2 \, ^{\circ}\text{C/min})$ of the solution (average size of crystal ~110 μ m). (d) An AC electric field $(1 \times 10^5 \, \text{V/m})$, frequency $= 10^6 \, \text{Hz}$) produces even finer grains (average size ~35 μ m). (e) Grain size vs frequency of AC field for different amplitudes. Fig. 7 reprinted with permission from Reference [103]. *Copyright: 2013 AIP Publishing LLC*.

charges. This section primarily focuses on studies where there is no externally applied electric field. Under such conditions, ice nucleation is influenced by free charge within the liquid or interfacial charges at a solid-liquid interface.

3.1. Influence of free charge in a liquid on freezing

Gabarashvili and Gliki [64] reported that supercooled water droplets containing charged impurities froze at higher temperatures for negatively charged droplets when compared to positive or no charge droplets. Hozumi et al. [72] proposed the formation of coordination compounds forming at the electrode as precursors for nucleation. Kramer et al. [104] measured the homogeneous nucleation rate for water droplets levitated in an electrodynamic Paul-trap and carrying varying amounts of charge. It was inferred that the homogeneous nucleation rate was unaffected by surface charge. Daniel et al. [81] carried out similar experiments in an electrodynamic balance and concluded that charges in the range \pm 4.2 \times 10⁻¹² C exert no influence on the freezing of supercooled water droplets. Furthermore, it was inferred that filamentation, induced on water droplets due to Coulomb instabilities occurring at Rayleigh limit failed to initiate nucleation.

3.2. Influence of surface charge on freezing

Pruppacher, in 1973 observed that supercooled droplets in contact with negatively charged sulphur particles froze at higher temperatures, and attributed this to the electric field in the vicinity of charged surfaces [60]. Subsequently, a majority of research in this area has involved measurements of surface charge-induced freezing on pyroelectric crystals. Pyroelectric materials generate electricity (flow of charge) when subject to an external temperature gradient. The underlying hypothesis [105–106] is that surface charges on pyroelectric crystals interact with interfacial water to create a structure conducive to the formation of ice. A pyroelectric crystal, when exposed to a temperature gradient of ΔT undergoes bulk polarization to induce an electric field (E) as [106]:

$$E = \frac{q}{\varepsilon_m \varepsilon_o} = \frac{\alpha \Delta T}{\varepsilon_m \varepsilon_o} \tag{2}$$

where, q is the surface charge per unit area, α is the pyroelectric coefficient, and $\varepsilon_m \& \varepsilon_o$ are the permittivities of the surrounding medium and vacuum respectively.

Furthermore, positively and negatively charged surfaces affect freezing differently [70,105,106]. This suggests that mechanisms other than the existence of an electric field are at play. Ehre et al. [105] studied freezing of supercooled water on charged surfaces of pyroelectric LiTaO₃ crystals and SrTiO₃ thin films. It was observed that positively and negatively charged surfaces facilitated and delayed freezing, respectively. The differences were attributed to the structural networks resulting from the different orientations of water molecules, with the oxygen and hydrogen molecules pointing towards the positively (oxygendown) and negatively (oxygen-up) charged surfaces [105–107]. These differences were explained via a molecular dynamics simulation, whereby the stacking of water layers (characteristic of the phase transition) was more pronounced for a positively charged surface than a negatively charged one [148].

Similar conclusions were reported by Belitsky et al. [106], wherein surface charge induced via the pyroelectric effect was shown to play a key role in inducing heterogeneous freezing. The proposed mechanism was a stabilization of a polar proton-ordered ice arrangement, due to the interaction of the positively charged surface with nearby polar water molecules. A similar mechanism was reported by Emmanuel [108,109], wherein sum frequency generation (SFG) spectroscopy measurements were employed to infer that ice crystals exhibit a proton-disordered arrangement next to a negatively charged surface, while the opposite is true for a positively charged surface (Fig. 8). Overall, it is evident that altering the structure and orientation of water molecules close to the surface by manipulation of surface charge or local electric fields profoundly influences freezing. Furthermore, freezing is enhanced for structural configurations in which the oxygen atoms in the water molecules are pointed towards the charged surface.

Table 2 summarizes the results of two key and detailed studies on this subject. Both studies conclusively show that surface charge influences the freezing temperature significantly. Furthermore, positively and negatively charged surfaces enhance and suppress freezing, respectively.

In a related study, Yang et al. [110] investigated the influence of surfaces modified with super charged unfolded polypeptides (SUPs) (resulting in charged surfaces) on ice nucleation. It was observed that surfaces modified with positively and negatively charged SUPs facilitated and suppressed ice nucleation respectively. This was attributed to the asymmetric polarization of water next to the charged surfaces, resulting in the formation of different structures of the interfacial water layer. Zhiyuan et al. [111] studied the influence of different ions on polyelectrolyte brush surfaces and reported that the effectiveness

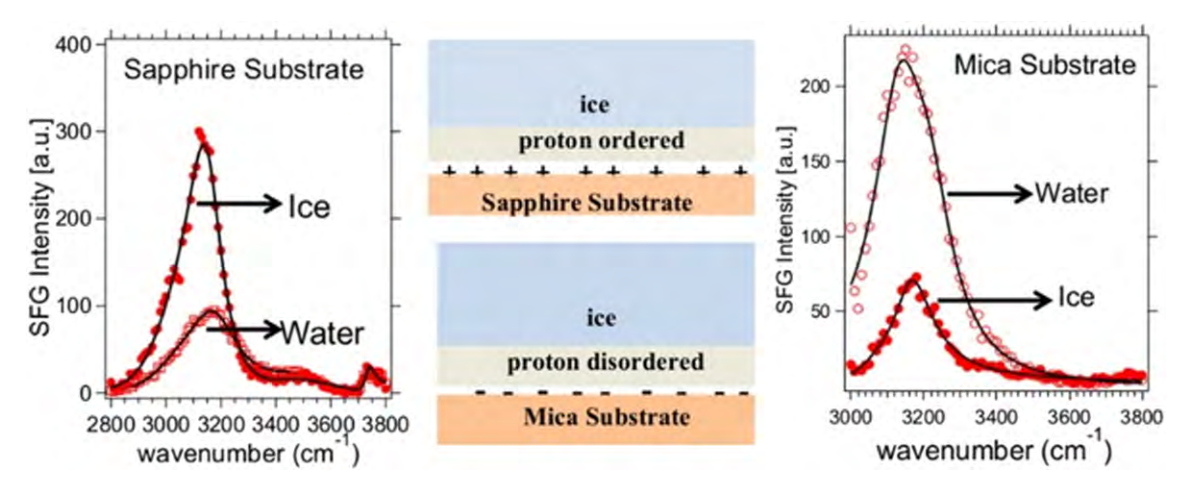


Fig. 8. Sum frequency generation (SFG) spectra of water on sapphire and mica substrates [109], illustrating the role of surface charge on freezing. The signal intensity of ice is greater than water for the positively charged sapphire surface. The reverse is true for a negatively charged mica surface. Figure reprinted with permission from Reference [109]. Copyright: 2016 American Chemical Society.

of ions in inducing nucleation closely followed the Hoffmeister series, which is a measure of the ability of ions to salt out proteins from a solution. This effect is, however, more pronounced for anions than cations. Accordingly, the nucleation temperature for various anions and cations exhibited the following order [111]:

$$SO_4^{2-} < F^- < Ac^- < HPO_4^{2-} < Cl^- < Br^- < SCN^- < NO_3^- < I^-$$

$$Ca^{2+}\!<\!Mg^{2+}\!<\!Gdm^{+}\!<\!K^{+}\!<\!Na^{+}\!<\!Cs^{+}\!<\!TMA^{+}\!<\!Li^{+}\!<\!NH_{4}^{+}$$

While the above studies conclude that positively and negatively charged surfaces enhance and suppress nucleation, respectively, Abdelmonem et al. [112] demonstrated via vibrational sum frequency generation (SFG) spectroscopy that the presence of any charged surface would suppress ice nucleation, irrespective of the polarity.

4. Analysis and simulations of electrofreezing

This section reviews current understanding of the various multiphysics phenomena underlying electrofreezing. This section is subdivided into two parts. The first part discusses the thermodynamic underpinnings of electrofreezing. The second part reviews molecular dynamics simulations-based studies of various aspects of electrofreezing.

4.1. Thermodynamic view of electrofreezing

As per classical thermodynamics, the probability that a system will undergo nucleation is dictated by the Gibbs free energy change (ΔG) of the system. Formation of a seed nuclei requires a negative change in the Gibbs free energy for the system undergoing a phase change $(\Delta G < 0)$. The net Gibbs free energy associated with nucleation typically has two components. The surface free energy (ΔG_s) is required to create a new solid-liquid interface of the nuclei. The second component is volumetric (ΔG_V) and is the free energy difference between the solid and liquid phases. Assuming a spherical shape for the solid cluster forming the ice nucleus, the volumetric free energy difference between the phases is:

$$\Delta G_V = \frac{4\pi r^3}{3} \Delta G_V \tag{3}$$

where, r is the radius of the spherical nuclei and ΔG_v is the free energy of transformation per unit volume. The term corresponding to the volumetric free energy difference (ΔG_v) is always negative and favors transformation; however, this is countered by the energy (ΔG_s) required to form a solid-liquid interface which is always positive.

$$\Delta G_{\rm S} = 4\pi r^2 \sigma \tag{4}$$

where σ is the surface energy per unit area of the liquid-vapor interface. In the presence of an electric field, an additional term, ΔG_F , which is

Table 2Summary of experimental studies on pyroelectricity-induced freezing.

Reference and year	Surface		Nucleation temperature (°C)	Significant findings
Belitzky et al. [106] w/ surface charge D,L-alanine		-2.5 ± 1.0	Surface charge elevates freezing temperature	
		L-aspartic acid	-5.0 ± 1.0	
		L-asparagine monohydrate $+$ 9 wt	-4.5 ± 1.0	
		%/wt L-aspartic acid		
		L-asparagine monohydrate	-8.0 ± 1.0	
	w/o surface charge	D,L-alanine	-5.5 ± 1.0	
		L-aspartic acid	-9.0 ± 2.0	
		L-asparagine monohydrate $+$ 9 wt	-8.5 ± 1.0	
		%/wt L-aspartic acid		
		L-asparagine monohydrate	-8.0 ± 1.0	
Ehre et al. [105]	w/ surface charge (positive)	LiTaO ₃	-7 ± 1.0	Positively and negatively charged surfaces
		SrTiO₃	-4 ± 1.0	enhance and suppress nucleation, respectively.
	w/ surface charge (negative)	LiTaO ₃	-18 ± 1.0	
		SrTiO₃	-19 ± 3.0	
	w/o surface charge	LiTaO ₃	-12.5 ± 3.0	
		SrTiO ₃	-12 ± 4.0	

Table 3Summary of melting properties of Ice Ih for different water models at 298 K and 1 bar. Note that the 3RT term for the melting enthalpy, arising from translational and rotational kinetics terms is not included. Data is extracted from References [118–140].

	SPC	SPC/E	TIP3P	TIP4P	TIP4P/Ew	TIP4P/2005	TIP4P/Ice	TIP5P	Experiments
Melting temperature (T _m) (K)	190	215	146	232	245.5	252.1	272.2	273.9	273.15
Density of liquid water (ρ_l) (g/cm ³)	0.991	1.011	1.017	1.002	0.992	0.993	0.985	0.987	0.999
Density of ice (ρ_{lh}) (g/cm^3)	0.934	0.95	0.947	0.94	0.936	0.921	0.906	0.967	0.917
Enthalpy of liquid (H1) (kcal/mol)	-11.64	-12.49	-11.69	-10.98	-12.02	-12.17	-13.31	-10.33	-
Enthalpy of ice (H _{Ih}) (kcal/mol)	-12.22	-13.23	-11.99	-12.03	-13.07	-13.33	-14.6	-12.08	-
Melting enthalpy ΔH_m (kcal/mol)	0.62	0.74	0.3	1.05	1.05	1.16	1.29	1.75	1.44
Slope of the coexistence curve (dp/dT) (bar/K)	-115	-126	-66	-160	-164	-135	-120	-708	-137

the free energy change due to the electric field is added to the analysis [78,83]. ΔG_E can be expressed as [78,113]:

$$\Delta G_{E} = -\frac{1}{2} \varepsilon_{o} \varepsilon_{water} \bigg(1 - \frac{\varepsilon_{ice}}{\varepsilon_{water}} \bigg) \bigg(2 + \frac{\varepsilon_{ice}}{\varepsilon_{water}} \bigg) V E_{in}^{2} \tag{5}$$

where, $\varepsilon_{\rm o}$ is the permittivity of vacuum, V is the volume of the critical nucleus, $\varepsilon_{\rm ice}$ and $\varepsilon_{\rm water}$ are the dielectric constants of ice and water respectively, and $E_{\rm in}$ is the internal electric field in water. The net free energy change accompanying ice nucleation in the presence of an electric field is thus:

$$\Delta G = \frac{4\pi r^3}{3} \Delta G_{v} + 4\pi r^2 \sigma - \frac{1}{2} \varepsilon_{o} \varepsilon_{water} \left(1 - \frac{\varepsilon_{ice}}{\varepsilon_{water}} \right) \left(2 + \frac{\varepsilon_{ice}}{\varepsilon_{water}} \right) V E_{in}^{2}$$
 (6)

An electric field thus manifests itself as a negative contribution to the overall Gibbs free energy. This provides a thermodynamic basis for nucleation promotion by an electric field. The Gibbs free energy can be related to the homogeneous nucleation rate, which can be experimentally measured.

According to classical nucleation theory [114–117], freezing follows the generation of solid nuclei in the liquid phase. Only nuclei above a critical size grow and induce crystallization in the liquid phase. Nucleation rate is the probability that such a critical nucleus will be formed per unit volume per unit time. The nucleation rate under homogeneous nucleation follows Poisson statistics and is expressed as [104,118]:

$$\frac{dN_u}{dt} = -J(t).V_d(t).N_u(t) \tag{7}$$

where, N_u is the number of unfrozen droplets at time t, J is the homogeneous nucleation rate, which depends on the temperature and electric field and V_d is droplet volume. Integrating this equation leads to:

$$\ln\left(\frac{N_u(t)}{N_0}\right) = -J(T).V_d.t \tag{8}$$

where, *No* is the sample size of the droplets investigated. Kashchiev [113] proposed an expression for the electric field-dependent

nucleation rate as:

$$J_N = J_N^0 \exp\left(\frac{\Delta G_E}{k_B T}\right) \tag{9}$$

where, J_N^0 is the nucleation rate in the absence of electric field, k_B is the Boltzmann constant and T is the temperature. The nucleation rate is related to the ratio of the number of unfrozen droplets to the total number of droplets as per Eq. (8) and is a measurable quantity which can be linked to the thermodynamic variables via Eq. (9). Similar analysis has been used to model the influence of the electric field and charge on the nucleation kinetics of supercooled water [104]. It should be noted that Eq. (8) and the resulting correlations are strictly valid only for homogeneous nucleation; analogous formulations need to be developed for heterogeneous nucleation.

4.2. Molecular Dynamics Simulations (MDS)

Molecular dynamics simulations (MDS) of various phenomena underlying electrofreezing has been an active research topic for the past two decades. A key theme analyzed in many studies is the role of an electric field in inducing spatial anisotropy and lowering the selfdiffusion activity of water molecules, thereby leading to a more ordered ice-like structure. The hydrogen bonding network in water also determines the freezing behavior, since the movement of water molecules is constrained by this network. The formation of a critical nucleus therefore strongly depends on the growth and collapse of the structural patterns of this network. Polarization induced by an electric field reduces the number of possible hydrogen-bonded structures feasible in liquid water, thereby inducing spatial anisotropy. However, a very high magnitude electric field O(10¹⁰) V/m would be required to induce an appreciable structural change in the cluster network. Such high electric fields cannot be externally applied in conventional experimental setups due to constraints such as the dielectric breakdown strength of liquid water. The upper limit on externally applied electric fields in experiments is only $O(10^6)$ V/m.

MDS are thus indispensable to understanding the structural behavior of the water network under the influence of high magnitude electric fields acting for very short time durations (order of picoseconds). Electric fields as high as 4 V/Å have been simulated in MDS studies which are at least three orders of magnitude higher than the electric

Table 4Summary of water monomer geometry and parameters for potential functions of different water models. It is noted that all models except for TIP5P place the negative charge at a point M, situated at a distance dom from the oxygen atom along the H-O-H bisector line. In the case of TIP5P, dol is the distance between oxygen and the L sites placed at the lone electron pairs. Data is extracted from References [118–140].

	SPC	SPC/E	TIP3P	TIP4P	TIP4P/Ew	TIP4P/2005	TIP4P/Ice	TIP5P
Distance between Oxygen and Hydrogen sites (d _{OH}) (Å)	1	1	0.9572	0.9572	0.9572	0.9572	0.9572	0.9572
H—O—H bond angle	109.47	109.47	104.52	104.52	104.52	104.52	104.52	104.52
LJ parameter σ (Å)	3.1656	3.1656	3.1506	3.154	3.1643	3.1589	3.1668	3.12
LJ parameter $\varepsilon/k_{\rm B}$ (K)	78.2	78.2	76.54	78.02	81.9	93.2	106.1	80.51
Charge on proton $q_H(e)$	0.41	0.423	0.417	0.52	0.524	0.5564	0.5897	0.241
Distance of negative charge from O along H-O-H bisector (d_{OM}) (Å)	0	0	0	0.15	0.125	0.1546	0.1577	_
Distance between the oxygen and the L sites placed at the lone electron pairs (d_{OL}) (\mathring{A})	-	_	-	-	-	-	-	0.7

Table 5Summary of molecular dynamics simulations of electrofreezing.

Reference and year	Focus of study	Methodology	Key results
Svishchev and Kusalik (1994) [138]	Influence of electric field on crystallization of water	• N = 256 (TIP4P) • T = 250 K	- Structural transition to cubic ice observed for electric fields between 0.1 and 0.5 V/Å $$
Xia and Berkowitz (1995) [147]	Effect of surface charge on structure of water between two Pt (100) surfaces	 E = 0.1-0.5 V/Å N = 512 (SPC/E) T = 300 K Parallelepiped unit cell with square base (L = 19.6 Å) 	 Increased surface charge results in stacking of water layers Crystallization of water lamina with intermediate domains of cubic ice observed at σ = 35.4
		• Surface charge densities (σ) = 0, 8.85, 26.55 & 35.4 × 10 ¹⁰ C/m ² corresponding to E = 0, 1, 3, 4 V/Å, respectively	$\times 10^{10} \text{C/m}^2$
Svishchev and Kusalik (1996) [139]	Effect of temperature, density & pressure on electrofreezing	• N = 64 & 256 (SPC/E & TIP4P) • T = 250 K	 TIP4P molecules in density range of 0.90–0.92 and 0.96–0.98 gcm⁻³ transformed into low and high density amorphous ice, respectively Threshold density for transformation of TIP4P molecules into cubic ice is between 0.94 and
Xia et al. (1995) [148]	Influence of electric field on the structure	• 3 pairs of simulations with $N = 512 \&$	0.96 gcm ⁻³ • Water molecules adsorbed next to surface
7.1d et al. (1555) [1 10]	of water confined between 2 platinum	1298 for Pt(100) & Pt(111) surfaces	(~1 nm) display solid state-like characteristics
	surfaces	 T = 300 K E = 0,1 and 2 V/Å 	 Molecules undergo structural transition to cubic ice under electric fields. Threshold field
		 Unit cell for Pt (100) surface: parallelepiped 	is 1–2 V/Å.
		with square base ($L = 19.6 \text{ Å}$)	• Dipolar saturation value of 80% at 1 V/Å increases
		 Unit cell for Pt (111) surface: parallelepiped with hexagon base (L = 2.24 nm) 	to 100% at 2 $V/\mbox{\normalfont\AA}$ indicating that cubic ice is formed at higher fields.
Borzsák, and	Effect of oscillatory shear and electric	• N = 256 (TIP4P, SPC/E)	Order of magnitude reduction in crystallization
Cummings (1997,	field on crystallization of supercooled	• T = 230 K	time at $E_{threshold} = 0.4$ –0.5 V/Å
1998) [143,144]	water	• $\rho = 1.17 \text{ g/cm}^3$	Effect of shear is more significant and crystallization is feater for SPC/F agent and to TIPAP model.
Yeh and Berkowitz	Influence of charged and uncharged Pt	 E = 0.1-1 V/Å N = 512 	is faster for SPC/E compared to TIP4P model. • Adsorbed water layer displays short-living
(1998) [163]	surfaces on dynamical properties of	• T = 300 K	hexagonal ice-like, and square lattice solid-like
, , , ,	interfacial water	• $E = 1-3 \text{ V/Å}$ corresponding to surface	structural characteristics, next to uncharged
		charge values of 8.85 and 26.65 μ C/cm ²	Pt(111) and Pt(100) surfaces, respectively.
		respectively.	Electric field leads to reorientation and layering
Jung et al. (1999)	Effect of electric field on structural	• <i>N</i> = 1000,256,125 (TIP4P);	transition.Number of 6 membered ring structures increases
[145]	characteristics of liquid water	• T = 363, 243-323 K	to 70–80% at $\rho=0.95~\&~1~gcm^{-3}$ for E = 0.5 V/Å • Threshold value of electric field to induce structural change is 0.15–0.2 V/Å
Sutmann (1998) [164]	Effect of electric field on structure and dynamics of water	 N = 200 (BJH) Simulation box: Cube of side 18.16 Å corresponding to ρ = 0.999 g/cm³ 	Transition to ice-like structure observed at room temperature for electric field of 4 V/Å
Vegiri and	Effect of electric field on dynamics of a	• N = 32 (TIP4P)	Structural transition related to partial ordering
Schevkunov (2001)	cluster of water molecules	• T = 200 K	into cubic forms observed at $E = 0.15 \text{ V/Å}$.
[166]		• E = 0.5-1 V/Å	 For E > 0.3 V/Å, proton disordered cubic forms appear and progressively become proton ordered at E = 1 V/Å
Alice Vegiri (2002)	Effect of electric field on single particle	• N = 32 (TIP4P)	Two critical electric fields corresponding to
[167]	translational dynamics and structural	• $T = 200 \text{ K}$	dipole polarization (1.5 \times 10 ⁹ V/m) and crystal
	transformation of water clusters parallel to field direction	• E = 0-0.7 V/Å	state transition (5 \times 10 9 V/m) identified
Zangi and Mark (2004) [157]	Effect of lateral electric field on confined water	• N = 1200 (TIP5P) • E = 0.5 V/Å	 Two different ice phases observed at T = 280 K for a confinement thickness corresponding to a trilayer: i) low density cubic ice consisting of hexagonal rings parallel to the wall, and ii) high
			density ice exhibiting an in-plane rhombic
A11 1711/000 11	Effects of all and C. I.I.	N 100 (TIP 17)	symmetry of O atoms.
Alice Vegiri (2004) [168]	Effect of electric field on structure and behavior of supercooled water	 N = 108 (TIP4P) T = 250 K. 	 Transition field strength corresponding to structural change is 10⁹ V/m for liquid and
[100]	beliavior of supercooled water	• $E = 0-0.15 \text{ V/Å}$	1.5×10^9 V/m for clusters
		,	• Electric fields $< 1.5 \times 10^9 \text{ V/m}$ can enhance
			liquid character of clusters; however no such
Van and Batass (2011)	Effect of local alectuic field	• N — 422 (I . I . 10 C Å I . 40 Å)	enhancement observed for bulk liquid.
Yan and Patey (2011) [149]	Effect of local electric field on heterogeneous nucleation of supercooled	• $N = 432$ (L _x = L _y = 19.6 Å, L _z = 40 Å), • $N = 1200$ (L _x = L _y = 32.68 Å, L _z = 40 Å)	 Electric fields exhibiting a functional variation with E_{max} ~0.5 V/Å, close to surface (~10 Å) in-
(= == 1	water	• $N = 1800 (L_x = L_y = 32.06 \text{ Å}, L_z = 40 \text{ Å})$ • $N = 1800 (L_x = L_y = 31.9 \text{ Å}, L_z = 60 \text{ Å})$	duce nucleation.
		 Six site model & TIP4P/ice model 	
		• $T = 270 \text{ K}$	
Eu et al. (2011) [150]	Effect of electric field an etweeting and	• $\rho = 0.96 \text{ g cm}^{-3}$	• Formation of pontagonal (F.O) balliant (F.1) and
Fu et al. (2011) [158]	Effect of electric field on structure and phase transition of water confined in a	 3.1 nm long SWCNT with d = 1.2 nm immersed in a cubic box 	 Formation of pentagonal (5,0), helical (5,1) and helical (5,2) ice nanotubes with application of an
	thick single walled carbon nanotube	• N = 46 (TIP4P)	electric field along tube axis.
	<u> </u>	• T = 230-350 K	• Threshold field at $T = 295$ K for first order solid
		• $E = 0-0.4 \text{ V/Å}$	to solid transition is $1.25 \times 10^9 V/m$ and 2.25

(continued on next page)

Table 5 (continued)

Reference and year	Focus of study	Methodology	Key results
Hu et al. (2011) [169]	Effect of electric field on structure and dynamics of water below glass transition temperature	 N = 1573 (Six site water potential) T = 77 K E = 0.05-4 V/Å Simulation box: Cube of side 3.6 nm 	 × 10⁹ V/m for transitions corresponding to (5,0) ↔ (5,1) and (5,1) ↔ (5,2) respectively. Two critical fields identified: Rapid onset of dipole polarization at 0.35 V/Å. Crystallization along with super polarization characterized by a potential energy minimum
Baranyai and Kiss (2011) [132]	Influence of electric field on water crystallization	• N = 432 (BK) • T = 250 K	at 4 V/Å • Critical electric field for crystallization is 0.35 V/Å
Hu et al. (2012) [170]	Combined influence of electric and magnetic fields on structure and dynamics of ice growth	 E = 0.01-2.5 V/Å TIP4P/2005 water models T = 240 K Electric (V/m)/magnetic fields (T) corresponding to 10⁶/0.01; 10⁷/0.1;10⁸/1 and 10⁹/10 Simulation box size dependent on specific 	• Combined influence of electric and magnetic fields is more effective in inducing ice growth at prismatic plane (10^6 V/m and 0.01 T) as against basal plane (10^9 V/m and 10 T)
Yan and Patey (2012) [150]	Influence of temperature, field strength and spatial range of electric field on ice nucleation	ice-water interface • TIP4P/Ice and six site water models with rectangular simulation cell. • T = 250-280 K (six site model); 245-270 K (TIP4P Ice)	 Threshold field strength to induce freezing for both models is E_{max} = 1.5 × 10⁹ V/m for c = 20 Å, where c represents spatial effectiveness of electric field. Higher threshold field strength (E_{max} corresponding to 2.5 × 10⁹ V/m for TIP4P/Ice and 3.5 × 10⁹ V/m for six site respectively) required for c = 10 Å.
Yan and Patey (2013) [151]	Effect of geometry and range of local electric fields on electrofreezing	 Six site & TIP4P water models T = 270 K Local electric field bands of varying range and geometry acting perpendicular to direction of slab geometry. 	 Ice nucleation commences at (111) plane of cubic ice Field band exceeding a threshold dimension initiates nucleation Shape of electric field bands gives qualitatively
Khusnutdinoff (2013) [171]	Influence of electric field on dynamics of hydrogen-bond network and structural ordering of water between graphene layers	 E_{max} = 0.3 V/Å Modified SPC/E_f potential Water molecules between graphene layers T = 280 K Electric fields and pressure ranging from 0 	similar results • Electric field >0.5 V/Å with pressure field induces structural ordering of water
Zhang et al. (2013) [161]	Influence of electric field on crystallization of water in a charged Pt nanochannel	 to 2 V/Å and 0-10 GPa N = 1250 (SPC/E) Water molecules sandwiched between 2 parallel Pt (111) plates with a charge density of +29 (top plate) and -29 (bottom plate) μC/cm². 	Surface layering of water enhanced with charged Pt(111) surfaces Water layered absorbed next to the Pt (111) surface suppresses nucleation of Ic and slows down growth of ice near surface
Qian et al. (2014) [172]	Influence of parallel electric field on structure and phase transition of water nanofilms confined between two graphene sheets	 T = 200 K TIP5P water molecules confined between 2 graphene sheets (4.9 × 4.9 nm²) separated by a distance of 1 nm T = 230 K 	• Water freezes and undergoes a first order solid-solid phase transition exhibiting properties similar to amorphous, hexagonal and rhombic bilayer ice for electric fields in the range of 0–0.2,
Zhang et al. (2014) [162]	Icing of water on polyethylene surfaces	 E = 0-0.15 V/Å N = 500 (SPC/E) confined between 2 PE (100/010) surfaces E = 3 V/Å T = 200 K Dimensions of simulation cell: (L_x = 12.965 Å, L_y = 19.716 Å, L_z = 110.164 Å) for (100) system & (L_x = 22.167 Å, L_y = 12.695, L_z = 100.066 Å) for (010) system 	 0.3–0.8 and 0.12–0.15 V/nm, respectively. (100) system: Ice nucleation promoted due to lattice match between quasi-ice layer (QIL) and bulk ice. (010) system: Structural deviation between QIL and bulk ice streamlined via a transition water layer in between
Zhang et al. (2014) [173]	Influence of electric field on structure and growth of ice	• N = 508 (SPC/E) • E = 0.4-4 V/Å • T = 200 K. • Dimensions of simulation cell (L _x = 0.6 Å, L _y = L _z = 0.2 Å)	 Density of resulting cubic ice increases from 0.98 to 1.08 gcm⁻³ with increasing field. Expedited crystal growth partially attributed to enhanced rotational dynamics due to electric field
Zhu et al. (2014) [174]	Electromelting to electrofreezing transition of water overlayer on a graphene surface as a function of surface charge	 N = 1320 (SPC/E) T = 300 K Surface charge (q) on graphene surface (98.4 × 93.72 Ų) increased from 0.00–0.18e 	 Transition of long range to short range order in radial distribution function observed at q between 0.06e to 0.07e, indicating a solid (ice I) to liquid transformation. Reverse transition (liquid to Ice II) observed for q between 0.12e and 0.13e Ice II found to have a structure commensurate to that of graphene. The underlying reason is the positive and negative values of Uw-w and Uw-g for q_c > 0.10e. Surface charge induces freezing by creating a structure commensurate to that of the base substrate.
Yan et al. (2014) [175]	Influence of external electric field on freezing of water	• N = 1000, 8000 & 32,000 (Six site model) • E = 0-0.2 V/Å	• Melting point increases by 24 K (at 0.1 V/Å) and 44 K (at 0.2 V/Å)

Table 5 (continued)

Reference and year	Focus of study	Methodology	Key results
Guo-Xi Nie et al. (2015) [159]	Effect of confinement on water solidification	 SPC/E T = 300 K E = 0-5 V/Å Separation between the plates: 1.2-4.4 nm 	Confinement hinders water solidification under external electric fields Parallel electric field more effective than perpendicular electric field in inducing crystallization
Druchok et al. (2015) [176]	Influence of electric field on structural changes in water	 N = 1600 (CF1) T = 298 K E = 0.025-0.25 V/Å Simulation box: cube of side 36 Å 	Critical electric field for crystallization is 0.25 V/Å
Mei et al. (2015) [177]	Effect of charged surfaces on bilayer of water confined in a nanoscale space	 N = 890 (TIP4P) T = 240 K Separation between charged walls = 0.95 nm 	 Transition between two types of ordered ice, governed by nanoconfinement (type I) and surface charge (type II) is observed. Transition characterized by intermediate liquid-like phase with maximum value of lateral in plane diffusion coefficient at a surface charge value of q_r = 0.5e.
Glatz and Sarupria (2016) [178]	Effect of surface charge distribution on ice nucleation on modified AgI surfaces	 N = 720 & 96 (on two slabs of Agl) (TIP4/Ice) T = 265 K Dimensions of simulation box: (L_x = 3.17 nm, L_y = 2.74 nm, L_z = 13.97 nm) 	Charged Agl surfaces with positively charged Ag atoms closer to water molecules (relative to negatively charged Ag) lead to a higher number of interfacial water molecules with orientations favorable for ice nucleation. Fastest ice nucleation observed for charge distribution and lattice structure similar to the ice bilayer formed on the surface.
Grabowska et al. (2017) [179]	Analysis of new ice layer formed on the basal and prism plane of a hexagonal ice crystal	 N = 1330 (TIP4P/Ice) T = 250-270 K 	 Local electric fields resulting from ordering of interfacial water molecules affect structure of the adhering ice layer. Formation of a hexagonal ice layer on the basal plane is preferred over cubic counterpart for supercooling >10 K Freezing rates higher on the prism plane when compared to a basal plane.

fields reported in experiments. This section discusses various aspects of MDS based studies relevant to electrofreezing; all such studies are summarized in Table 5. It is noted that in-depth analyses on various water models used in the simulations, and their appropriateness in replicating the properties of water and ice has been discussed in many studies [118–140], and is not reviewed presently. However, for the sake of completeness, we have summarized the key melting and structural properties of these water models in Tables 3 and 4.

4.2.1. Effect of an electric field on molecular structure of bulk water

While it was possible to study crystallization of monoatomic liquids via MDS in the later part of the twentieth century, molecular liquids were usually observed to be trapped in metastable glassy states, only emerging for cases of slow reduction in temperatures. This hampered the detection of a heterophase nucleus within the timescale of typical simulations [138]. However, it was observed that polar molecular liquids like water can nucleate from the metastable phase with the assistance of an electric field, thereby making it possible to study crystallization of water through simulations [139–141].

Svishchev and Kusalik [138] were the first to report electrofreezing of water through MDS in 1994. It was inferred from a study of the oxygen–oxygen radial distribution function that a morphological transition of liquid water into cubic ice can be achieved at a threshold field between 0.1 and 0.5 V/Å with a transition time on the order of 200 ps. The cubic structure (by virtue of its diamond-type lattice packing arrangement) enables a favorable parallel arrangement of the molecular dipoles with respect to the electric field direction, the result of which is a dipole saturation value of almost 90%. This explains the transformation into cubic ice as against the more commonly existing hexagonal ice. Importantly, the electric fields in this simulation were similar in magnitude to local electric fields existing near surfaces (molecular level distance) of certain biopolymers [142], or within the cracks of amino acid crystals [70].

Furthermore, Svishchev and Kusalik [140] reported that TIP4P molecules failed to crystallize at water simulation cell densities ranging from 0.9-0.92 and 0.96-0.98 g/cm³, but instead transformed into low and high-density amorphous ice, respectively at 250 K. The threshold density range for crystallization into cubic ice was estimated to be between 0.94 and 0.96 g/cm³. SPC/E molecules displayed a lower propensity for nucleation by crystallizing at 220 K for a field strength of 0.7 V/Å and density of 0.98 g/cm³ at a time scale of 350 ps. It is noted that the melting point of SPC/E water model (200K) is lower than that of TIP4P water model (240 K). Constant density simulations were more effective than constant pressure simulations in producing good polar ice crystals. Shortly thereafter, it was observed [139] that applying an electric field to TIP4P water at a pressure of 3-5 kilobar and at temperatures ranging from 225 to 240 K led to the formation of a hitherto unknown open quartz-like structure at timescales of 1 ns; this was denoted as ice XII.

It was established by Svishchev and Kusalik [140] that complete polarization of molecules necessitates a break-up of hydrogen bonds between adjacent molecular layers; this is achieved via electric fields. Borzsak [143,144] reported that an oscillatory shear mechanism in the form of a planar Couette flow assists electric fields in enhancing electrofreezing. This is achieved by distorting the network of hydrogen bonds, thereby assisting polarization of the molecules with the aid of an electric field in an effective manner. It is noted that oscillatory shear was applied only during the first 200 ps of the simulations, as any further application could cause the crystalline structure to be sheared off. The use of oscillatory shear reduced the simulation times by an order of magnitude, thereby expediting the formation of the conjectured ice XII polymorph [139] at high pressures, and facilitating cubic ice formation at ambient pressure.

Jung et al. [145] studied the influence of an electric field on the molecular structure of liquid water. It was inferred that at 243 K, an electric field of $0.5\ V/\text{Å}$ results in an increase in the number of six-membered

ring structures, accompanied by a simultaneous decrease of other ring structures. Since Ice I structure is predominantly composed of sixmembered rings [140], the resulting structure was inferred to be that of ice I_c as depicted in Fig. 9 (a, b).

4.2.2. Effect of charged surfaces or local electric fields on interfacial water molecules

The structural transition of interfacial water molecules adjacent to charged surfaces or under the influence of electric fields is the subject of many MDS-based studies. The primary focus is to capture the dependence of the dynamical evolution of structural characteristics of the phase transition on surface charge and electric field [146–151]. Xia and Berkowitz [147] conducted simulations for a system of 512 SPC/E water molecules confined between two Pt (100) surfaces with opposite surface charges. Key findings are as follows:

- Density profile graphs indicated that an increase in the magnitude of surface charge had an effect on density distribution of H and O atoms, leading to a stacking of water layers, in proportion to the magnitude of surface charge. This effect was more pronounced for water layers close to the positively charged surface (Fig. 10(a)).
- Water dipoles displayed an orientation preference with increasing surface charge, with almost 100% dipole polarization for a surface charge density of 35.4 × 10¹⁰C/m².
- At a surface charge of 35.4×10^{10} C/m², the water lamina between the surfaces underwent significant stacking, characteristic of transformation into a crystalline structure, with intermediate domains of strained cubic ice lattices.

Yan and Patey [149] studied heterogeneous nucleation of supercooled water under the influence of electric fields ($E_{\rm max}=5\times10^9~{\rm V/m}$) acting very close (within 10 Å of the surface), and in a direction parallel to that of the surface. Formation of a thin ordered layer of water, very close to the surface was observed, which acts as an ice nucleant with structural properties similar to that of dipole-ordered cubic ice. Ice nucleates on the outer edge of this layer and grows into the bulk of the liquid. Yan and Patey [159] further conducted quantitative analysis on local surface-field induced ice nucleation [150], and the geometry and range specific effects of local electric field bands on ice nucleation [151]. It was observed that electric fields which remain effective at greater distances away from the surface (subject to a threshold distance) lead to stronger polarization; this reduces the magnitude of

the field required to induce freezing. Furthermore, ice growth always commenced at the (111) plane of cubic ice.

Zhu et al. [174] observed that increasing the magnitude of charge on a graphene surface increases the interaction energy between water and graphene ($U_{w\,-\,g}$), and simultaneously decreases the water-water ($U_{w\,-\,w}$) interaction energy. The lower attractive forces between water molecules lead to electromelting of the ice previously formed on the surface of graphene. Furthermore, above a critical charge limit, $U_{w\,-\,g}$ and $U_{w\,-\,w}$ switch signs, becoming negative and positive respectively, thereby indicating attractive and repulsive forces, respectively. This leads to freezing of electromelted water due to the creation of a structure commensurate to that of graphene (since $U_{w\,-\,g} < 0$). Overall, surface charge can induce freezing by creating a structure commensurate with that of the base substrate, by increasing the interaction energy between water and the base substrate.

4.2.3. Confinement-induced solidification

While Xia and Berkowitz [147] (Section 4.2.2) studied the influence of surface charge on water confined between two plates (spacing ~40 Å) carrying equal and opposite charge, this section examines studies on the behavior of water under smaller confinements, approaching a few molecular layers (typically 8–12 Å). Multiple studies [152–157] report that liquid water (unlike other molecular liquids) does not crystallize upon confinement at room temperatures. However, confinement, coupled with an electric field accelerates freezing [157] by restricting the orientational degrees of freedom of molecular dipoles along axes perpendicular to the direction of the electric field. This translates to a reduced entropy contribution to the free energy of the liquid-solid phase transition, thereby assisting crystallization.

Zangi and Mark [157] studied electrofreezing for a system of 1200 TIP5P water molecules confined in a slab-like configuration between two parallel plates, and subject to a lateral electric field of 0.5 V/Å. For a plate separation distance equal to the thicknesses of a tri-layer of water molecules (0.92 nm), two distinct phases of ice (low and high density) were found to exist at 280 K. The low-density and high-density ice phases displayed in-plane hexagonal and rhombic symmetry, respectively. Furthermore, the degree of ordering exhibited an inverse dependence on the plate distance.

Fu et al. [158] investigated the phase transition of water confined in a single-walled carbon nanotube (diameter: 1.2 nm), under the influence of an electric field applied along its axis. They reported the

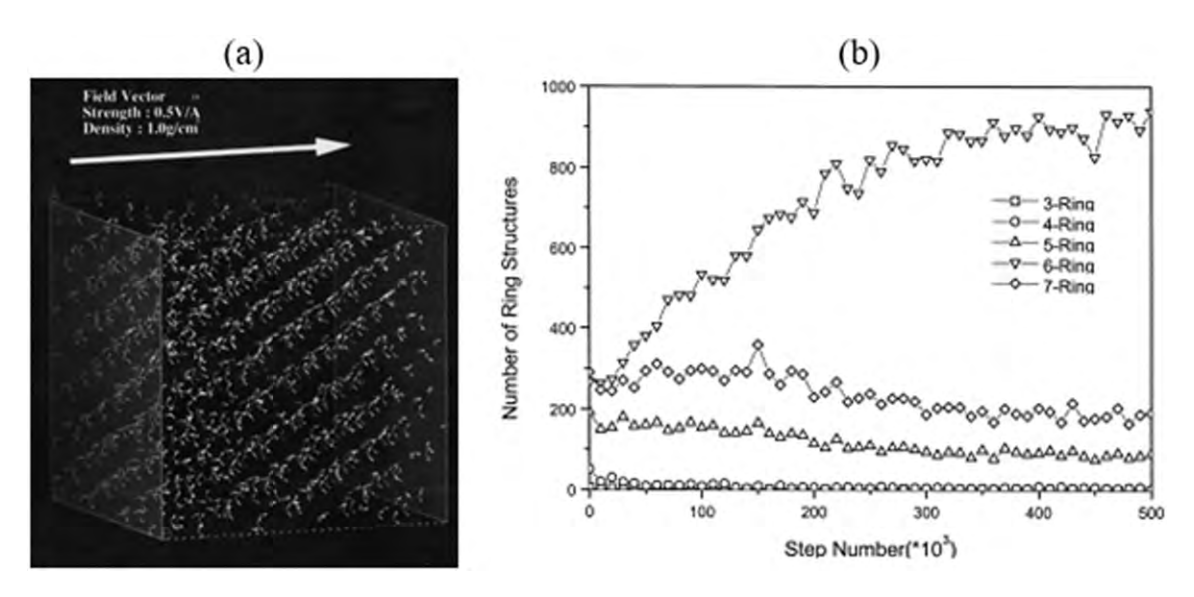


Fig. 9. (a) Structural change induced in liquid water ($\rho = 1 \text{ g/cm}^3$) at 243 K and an electric field of 0.5 V/Å [145]. (b) Variation in the number of different membered ring structures during the course of the simulation [145]. Fig. 9 (a) & (b) reprinted with permission from Reference [145]. *Copyright: 1999 Elsevier*.

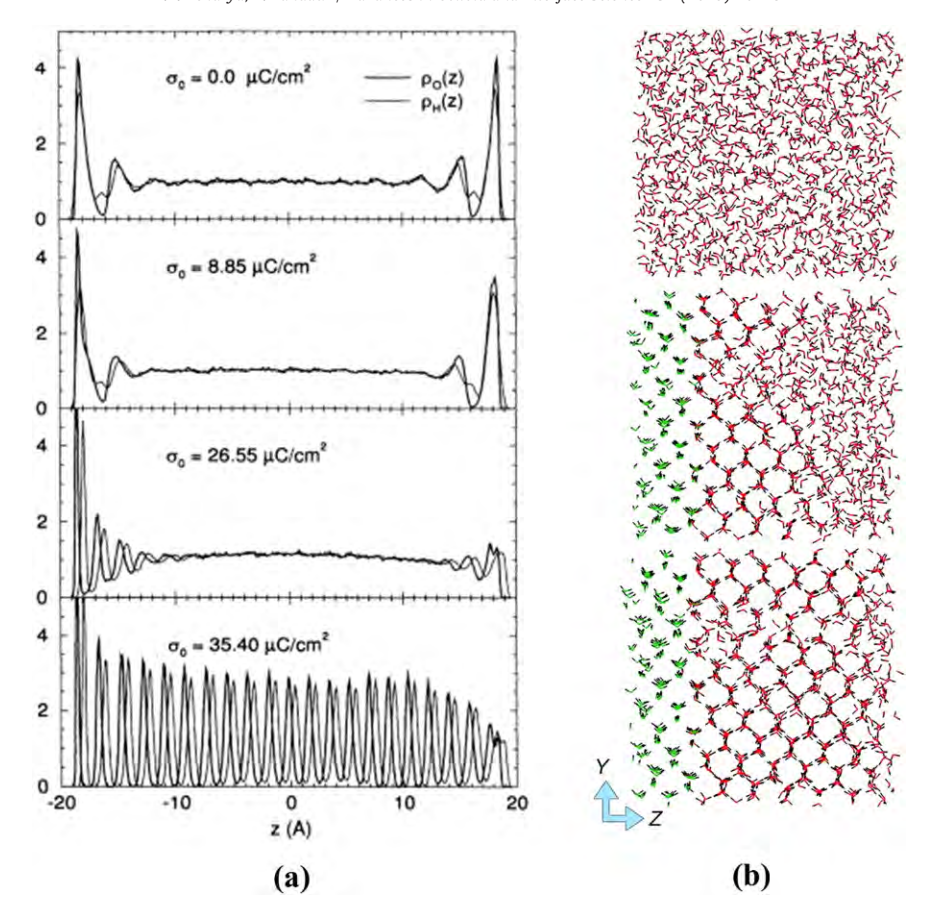


Fig. 10. (a) Normalized density distribution plots of oxygen and hydrogen atoms for increasing surface charge with the left and right surfaces positively and negatively charged, respectively. Significant stacking of water layers occurs with increasing surface charge [147] (b) Configurational snapshot of electrofreezing simulation for localized electric field [149]. The field is applied along the Y-axis with the three panels representing snapshots at t = 0, 2.4 & 4 ns starting from top to bottom. Oxygen atoms of the water molecules that experience the field (z ≤ 10 Å) are green, those outside the field region are red. Hydrogen atoms are denoted in black. Fig. 10 (a) reprinted with permission from Reference [147]. Copyright 1995 American Physical Society. Fig. 10 (b) reprinted with permission from Reference [149]. Copyright: 2011 American Chemical Society.

formation of pentagonal (5,0) and a hitherto unreported helical (5,1) and (5,2) ice nanotubes from liquid water. The liquid to solid transition into either of these geometries was seen to depend on the magnitude of the electric field.

The above studies observed crystallization due to confinement in the presence of an electric field. Conversely, Guo-Xi Nie et al. [159], observed that confinement at the nanoscale hinders water solidification under external electric fields. Additionally, a parallel electric field was more effective in inducing water solidification when compared to a perpendicular electric field. Similarly, it was reported by Hu and Wanlin [160], that an electric field could induce melting in confined monolayer ice. The critical melting temperature of confined monolayer ice was found to decrease with increased field strength.

4.2.4. Benchmarking MDS-based studies

This section begins by highlighting a link between the observations of MDS-based studies and the 'theory of disordered layers', proposed decades earlier (1970) by Evans [61]. Evans proposed that freezing commences on a layer of interfacial water molecules firmly adsorbed on a solid surface and that the dynamics of ice nucleation can be tuned by modulating the properties of this interfacial water layer. As an illustration, Yan & Patey [149], observed the formation of a thin ordered layer of water next to the surface in the presence of local electric fields; this acts as a precursor upon which layers of ice nucleate and propagate into the bulk. Similarly, Xia and Berkowitz [147] reported that water molecules next to a platinum surface display solid-like characteristics. However, it was reported by Zhang et al. [161] that the presence of the

water layer, adsorbed to the surface in a charged platinum nanochannel impedes the growth of cubic ice I_c, and slows ice growth near surfaces.

Evans' theory was further substantiated in a study by Zhang et al. [162] on electrofreezing of water on polyethylene surfaces. It was observed that a surface film composed of 3–4 molecular layers of water was formed next to the solid surface. Furthermore, ice nucleation dynamics was determined by the two layers closest to the surface, termed as the quasi-ice layer (QIL). It was reported that a similarity in the lattice structure of QIL and ice promotes nucleation in the event of slight deviations in the lattice structures of the solid surface [polyethylene (100)] and ice. This directly corroborates Evans' hypothesis proposed four decades earlier. Additionally, any dissimilarity in the lattice structure of QIL and ice could be relaxed by a transition layer of water molecules between QIL and bulk ice. Similarly, Yeh and Berkowitz [163] observed that water layers adsorbed next to platinum (111) and (100) surfaces adopt hexagonal ice and square lattice solid like structural characteristics respectively.

It is important to note the discrepancies in the values of the critical electric field for crystallization of water. These can be attributed to different models and the size and geometry of simulation cells utilized in these studies. Jung et al. [145] observed crystallization for electric fields ranging from 0.15–0.2 V/Å (TIP4P), whereas Sutmann [164] and Xia et al. [148] observed crystallization for electric fields between 4 V/Å (BJH) and 1–2 V/Å (SPC/E) respectively. Yeh and Berkowitz [165] and Svishchev and Kusalik [139] however, reported crystallization at an electric field (E_T) between 0.5 and 1 V/Å (SPC/E) and 0.1–0.5 V/Å (TIP4P) respectively. This is the total electric field (E_T) where, E_T = E_X + E_P and ϵ = E_X/E_T. E_X, E_P and ϵ are the applied electric field,

electric field due to internal polarization and the dielectric constant, respectively. It is important to note that in simulations involving a water slab utilizing 2-D Ewalds summation technique, the value of E_T emerges from simulation data (i.e. E_T is not equal to E_X), whereas for bulk simulations utilizing 3-D Ewalds summation technique, E_T equals the applied electric field (E_X) [165].

5. Conclusions and future outlook

Various fundamental mechanisms underlying electrofreezing have been systematically classified and critically reviewed. It is seen that electrofreezing can enhance ice nucleation significantly. Best results to date include freezing at a supercooling of only 0.1 °C [71], and a 16 °C elevation [83] in the nucleation temperature (compared to the no electrofreezing case). Over the last few decades, various mechanisms have been studied including molecular rearrangements of water near the surface, contact line dynamics, electrochemistry-related effects, confinement, bubble-related mechanistic effects etc. While all these effects play a role, their relative importance in complex systems is not well understood and deserves further attention. Our understanding of electrofreezing will also benefit from a better synergy between MDS-based studies and experimental efforts. MDS can study the reorganization of molecular volumes of liquid water under high magnitude electric fields for short time durations and has confirmed some previous hypothesis on possible mechanisms. Yet, MDS-based results cannot often be validated directly via experiments, wherein the maximum electric field is limited by practical considerations, and nucleation detection at molecular-level length scales remains a challenge. To conclude, while there has been significant progress in our understanding of electrofreezing, there remain unanswered questions about molecular level mechanisms, as well as macroscopic aspects of electrofreezing.

Acknowledgements

The authors acknowledge National Science Foundation CBET-1653412, American Chemical Society Petroleum Research Fund PRF 54706-DNI5 and Welch Foundation Grant # F-1837 for supporting this work.

References

- [1] Pruppacher HR, Klett JD. Microphysics of clouds and precipitation. 2nd rev. ed. Dordrecht: Kluwer Academic; 1997.
- Murray BJ, O'Sullivan D, Atkinson JD, Webb ME. Chem Soc Rev 2012;41(19): 6519-54.
- [3] Baker MB. Cloud microphysics and climate. Science 1997;276:1072.
- [4] Rzesanke D, Duft D, Leisner T. Climate and weather of the sun-earth system (CAWSES). Netherlands: Springer; 2013; 89-107.
- Tennakone K. Int J Theor Phys 2012(s(4)):1013-21.
- [6] Tinsley BA. J Geomagn Geoelectr 1991;43(Supplement 2):775-83.
- [7] Ahmad S, Yaghmaee P, Durance T. Food Bioprocess Technol 2012;5(3):1019–27.
- [8] Delgado AE, Zheng L, Sun DW. Food Bioprocess Technol 2009;2(3):263-70.
- [9] Ming LC, Rahim RA, Wan HY, Ariff AB. Food Bioprocess Technol 2009;2(4):431.
- [10] Streit F, Corrieu G, Béal C. Food Bioprocess Technol 2010;3(1):36-42.
- [11] Yu S, Ma Y, Zheng X, Liu X, Sun DW. Food Bioprocess Technol 2012;5(1):391-400.
- [12] Saclier M, Peczalski R, Andrieu J. Chem Eng Sci 2010;65(10):3064-71.
- [13] Laakso T, Holttinen H, Ronsten G, Tallhaug L, Horbaty R, Baring-Gould I, et al. Stateof-the-art of wind energy in cold climates. VTT, Finland: IEA Wind Annex XIX; 2003.
- [14] Sun CQ, Sun Y. Electrofreezing and water bridging. The attribute of water. Singapore: Springer; 2016. p. 393-418.
- [15] Moore EB, Molinero V. Nature 2011;479(7374):506-8.
- [16] Petrenko VF, Whitworth RW. Physics of ice. OUP Oxford; 1999.
- [17] Fletcher NHJ. J Chem Phys 1958;29(3):572-6.
- [18] Zhu H, Guo Z, Liu W. Chem Commun 2014;50(30):3900-13.
- [19] Antonini C, Innocenti M, Horn T, Marengo M, Amirfazli A. Cold Reg Sci Technol 2011:67(1):58-67
- [20] Alizadeh A, Yamada M, Li R, Shang W, Otta S, Zhong S, et al. Langmuir 2012;28(6): 3180-6.
- [21] Alizadeh A. Bahadur V. Zhong S. Shang W. Li R. Ruud I. et al. Appl Phys Lett 2012: 100(11):111601
- [22] Varanasi KK, Deng T, Smith JD, Hsu M, Bhate N. Appl Phys Lett 2010;97(23):234102.
- [23] Farhadi S, Farzaneh M, Kulinich SA. Appl Surf Sci 2011;257(14):6264–9.
- [24] Kulinich SA, Farzaneh M. Appl Surf Sci 2009;255(18):8153-7.

- [25] Alizadeh A. Bahadur V. Kulkarni A. Yamada M. Ruud IA. MRS Bull 2013:38(05): 407-11
- [26] Kasper JC, Friess W, Eur J Pharm Biopharm 2011;78(2):248-63.
- [27] Murray BJ, O'sullivan D, Atkinson JD, Webb ME. Chem Soc Rev 2012;41(19): 6519-54.
- [28] Cantrell W. Heymsfield A. Bull Am Meteorol Soc 2005;86(6):795-807.
- [29] Vali G, Kulmala M, Wagner P. Ice nucleation—a review. Nucleation and atmospheric aerosols, Elsevier: 1996, p. 271-9.
- [30] Pruppacher HR. Zeitschrift für Angewandte Mathematik und Physik (ZAMP) 1963; 14(5):590-9.
- [31] Vali C. I Rech Atmosph 1985:19(2-3):105-15
- [32] Laaksonen A, Talanquer V, Oxtoby DW. Annu Rev Phys Chem 1995;46(1):489–524.
- [33] Szyrmer W, Zawadzki I. Bull Am Meteorol Soc 1997;78(2):209–28.
- [34] Martin ST, Chem Rev 2000:100(9):3403-54.
- [35] DeMott PJ. Laboratory studies of cirrus cloud processes. Univ. Press: Oxford; 2002; 102-35
- [36] Woo MW, Mujumdar AS. Dry Technol 2010;28(4):433-43.
- [37] Geidobler R, Winter G. Eur J Pharm Biopharm 2013;85(2):214-22.
- Cheng L, Sun DW, Zhu Z, Zhang Z. Crit Rev Food Sci Nutr 2017;57(4):769-81.
- [39] Hammadi Z, Veesler S. Prog Biophys Mol Biol 2009;101(1):38-44.
- [40] Dalvi-Isfahan M, Hamdami N, Xanthakis E, Le-Bail A. J Food Eng 2017;195:222–34.
- [41] Dalvi-Isfahan M, Hamdami N, Le-Bail A, Xanthakis E, Food Res Int 2016;89:48–62.
- Kiani H, Sun DW. Trends Food Sci Technol 2011;22(8):407-26.
- [43] James C, Purnell G, James SJ. Food Bioprocess Technol 2015;8(8):1616-34.
- [44] Morris GJ, Acton E. Cryobiology 2013;66(2):85–92.
- [45] Anuj G. Int J Drug Dev Res 2012;4(3):35-40.
- [46] Misra NN, Koubaa M, Roohinejad S, Juliano P, Alpas H, Inácio RS, et al. Food Res Int 2017:97:318-39
- [47] Jha PK, Sadot M, Vino SA, Jury V, Curet-Ploquin S, Rouaud O, et al. Innovative Food Sci Emerg Technol 2017;42:204-19.
- [48] Nanev CN. Crystals 2017;7(10):310.
- Jha PK, Xanthakis E, Jury V, Le-Bail A. Crystals 2017;7(10):299.
- [50] Dufour L. Ann Phys Rehabil Med 1862;190(12):530-54.
- [51] Farzaneh M. Philos Trans R Soc Lond A: Math Phys Eng Sci 2000;358(1776): 2971-3005.
- Schaefer V. Project Cirrus, Final Rept. Schenectady, New York: General Electric Research Laboratory; 1953; 52-3.
- [53] Pruppacher H. J Geophys Res 1963;68:4463-74.
- [54] Loeb LB. J Geophys Res 1963;68:4475.
- [55] Loeb LB, Kip AF, Einarsson AW. J Chem Phys 1938;6:264–73.
- [56] Abbas MA, Latham J. Journal of the Meteorological Society of Japan Ser II 1969; 47(2):65-74.
- Koenig LR. J Atmos Sci 1965;22(4):448-51.
- Goyer GG, Watson RD. Report in appendix IV of final report fourth Yellowstone field research expedition. Pub. No. 22. Atmospheric Sciences Research Center, State University of New York, Albany; 1964.
- [59] Smith MH, Griffiths RF, Latham J. Q J R Meteorol Soc 1971;97(414):495-505.
- [60] Pruppacher HR. Pure Appl Geophys 1973;104(1):623–34.
- [61] Evans LF. The role of the adsorbed layer in ice nucleation. Preprint Conf. Cloud Physics, Am. Meteor. Soc., Fort Collins; 1970 (January)
- [62] Rau W. Zeitschrift für Naturforschung A 1951;6(11):649-57.
- Salt RW. Science 1961;133(3451):458-9.
- [64] Gabarashvili TG, Gliki NV. Izvestiya Acad. Sci: USSR. Atmos Oceanic Phys 1967;3:
- [65] Dawson GA, Cardell GR. J Geophys Res 1973;78(36):8864-6.
- [66] Doolittle JB, Vali G, J Atmos Sci; 32(2): 375-379.
- [67] Shichiri T, Nagata T. J Cryst Growth 1981;54(2):207-10.
- [68] Sivanesan S, Gobinathan R. Mater Chem Phys 1991;27(4):385-92.
- [69] Shichiri T, Araki Y. J Cryst Growth 1986;78(3):502-8.
- [70] Gavish M, Wang J-L, Eisenstein M, Lahav M, Leiserowitz L. Science 1992;256(5058):
- [71] Braslavsky I, Lipson SG. Appl Phys Lett 1998;72(2):264-6.
- [72] Hozumi T, Saito A, Okawa S, Watanabe K. Int J Refrig 2003;26(5):537–42.
- [73] Hozumi T, Saito A, Okawa S, Eshita Y. Int J Refrig 2005;28(3):389-95.
- [74] Choi EM, Yoon YH, Lee S, Kang H. Phys Rev Lett 2005;95(8):085701.
- [75] Kotodziej HA, Jones GP, Davies M. J Cheml Soc Faraday Trans 2: Molec Chem Phys 1975;71:269-74.
- [76] Song C, Wang P. Rev Sci Instrum 2010;81(5):054702.
- [77] Landau LD, Lífshíts EM, Pitaevskii LP. Electrodynamics of continuous media. Vol. 8. Oxford: Pergamon press; 1984(pp. 153-157)
- [78] Stan CA, Tang SK, Bishop KJ, Whitesides GM. J Phys Chem B 2010;115(5):1089-97.
- [79] Mugele F, Baret JC. J Phys Condens Matter 2005;17(28):R705.
- [80] Nakajima A, Imase A, Suzuki S, Yoshida N, Sakai M, Hashimoto A, et al. Chem Lett 2007;36(8):1020-1.
- [81] Rzesanke D, Nadolny J, Duft D, Müller R, Kiselev A, Leisner T. Phys Chem Chem Phys 2012:14(26):9359-63.
- [82] Yang F, Shaw RA, Gurganus CW, Chong SK, Yap YK. Appl Phys Lett 2015;107(26):
- [83] Carpenter K, Bahadur V. Langmuir 2015;31(7):2243-8.
- [84] Carpenter K, Bahadur V. J Phys Chem Lett 2016;7(13):2465–9.
- [85] Shahriari A, Acharya PV, Carpenter K, Bahadur V, Langmuir 2017;33(23):5652-6. [86] Wei S, Xiaobin X, Hong Z, Chuanxiang X, Cryobiology; 56(1): 93-99.
- [87] Orlowska M, Havet M, Le-Bail A. Food Res Int 2009;42(7):879-84.
- [88] Doolittle JB, Vali G. J Atmos Sci 1975;32(2):375-9.
- [89] Ma Y, Zhong L, Zhang H, Xu C. Solid dielectrics (ICSD), 10th IEEE International Conference, July 2010, IEEE; 2010; 1-4.

- [90] Jankowski NR. McCluskev FP. Proc. 14th international heat transfer conference IHTC, Washington DC, August 7–13 2010. Am Soc Mech Eng 2010;7:409–16.
- Zhang XX, Li XH, Chen M. Atmos Res 2016;178:150-4.
- [92] Wilson PW, Osterday K, Haymet ADJ. CryoLetters 2009;30(2):96–9. [93] Petersen A, Rau G, Glasmacher B. Heat Mass Transf 2006;42(10):929–38.
- [94] Hindmarsh IP, Russell AB, Chen XD, I Food Eng 2007;78(1):136-50.
- [95] Nakagawa K, Hottot A, Vessot S, Andrieu J. Chem Eng Process Process Intensif 2006; 45(9):783-91.
- [96] Chevalier D, Le Bail A, Ghoul M. J Food Eng 2000;46(4):287–93.
- [97] Chevalier D, Sequeira-Munoz A, Le Bail A, Simpson BK, Ghoul M. Innovative Food Sci Emerg Technol 2000;1(3):193-201.
- Zhu S, Bail A, Ramaswamy HS, Chapleau N. J Food Sci 2004;69(4).
- [99] Kim SC, Shin JM, Lee SW, Kim CH, Kwon YC, Son KY, Non-freezing refrigerator. Patent no. WO2007/094556A2, 2007 (International Patent).
- Sun W, Xu X, Sun W, Ying L, Xu C. Properties and applications of dielectric materials. 8th International Conference. IEEE; 2006. p. 774–7.
- [101] Sun W, Li XH. Proc. 3rd international congress, image and signal processing (CISP), Yantai China. 16–18 October 2010. . 6IEEE: 2010 October: 2933–6.
- [102] Yahong M, Lisheng Z, Huiyu H, Qinxue Y, Yewen Z. Properties and applications of dielectric materials (ICPADM), IEEE 10th International Conference, July 2012. IFFF: 2012: 1-4
- [103] Ma Y, Zhong L, Gao J, Liu L, Hu H, Yu Q. Appl Phys Lett 2013;102(18):183701.
- [104] Krämer B, Hübner O, Vortisch H, Wöste L, Leisner T, Schwell M, et al. J Chem Phys 1999:111(14):6521-7.
- [105] Ehre D, Lavert E, Lahav M, Lubomirsky I. Science 2010;327:672-5.
- [106] Belitzky A, Mishuk E, Ehre D, Lahav M, Lubomirsky I. J Phys Chem Lett 2016;7:43-6.
- [107] Toney MF, Howard JN, Richer J, Borges GL, Gordon JG, Melroy OR, et al. Nature 1994:368(6470):444-6.
- [108] Anim-Danso E, Zhang Y, Alizadeh A, Dhinojwala A. J Am Chem Soc 2013;135: 2734-40.
- [109] Anim-Danso E, Zhang Y, Dhinojwala A. J Phys Chem C 2016;120(7):3741-8.
- [110] Yang H, Ma C, Li K, Liu K, Loznik M, Teeuwen R, et al. Adv Mater 2016;28(25): 5008-12
- [111] He Z, Xie WJ, Liu Z, Liu G, Wang Z, Gao YQ, et al. Sci Adv 2016;2(6):1600345.
- [112] Abdelmonem A, Backus EH, Hoffmann N, Sánchez MA, Cyran JD, Kiselev A, et al. Atmos Chem Phys 2017;17:7827-37.
- Kashchiev D. Philos Mag 1972;25(2):459-70.
- [114] Frenkel J. Kinetic theory of liquids., 8New York: Dover Publ; 1955; 143.
- [115] Farley FJM. Proc R Soc Lond 1952; Ser. A, 212:530.
- [116] Turnbull D, Fisher JC. J Chem Phys 1949;17(1):71-3.
- [117] Zeldovich J. Sov Phys JETP 1942;12:525. [118] Laird BB, Haymet ADJ. Chem Rev 1992;92(8):1819–37.
- [119] Karim OA, Haymet ADJ. J Chem Phys 1988;89(11):6889–96.
- [120] Poole PH, Essmann U, Sciortino F, Stanley HE. Phys Rev E 1993;48(6):4605.
- [121] John ST, Klein ML. Phys Rev Lett 1987;58(16):1672.
- [122] Abascal JLF, Sanz E, Garcia Fernandez R, Vega C. J Chem Phys 2005;122(23):234511.
- [123] Abascal JL, Vega C. J Chem Phys 2005;123(23):234505.
- [124] Mahoney MW, Jorgensen WL. J Chem Phys 2000;112(20):8910-22.
- [125] Vega C, Abascal JL, Conde MM, Aragones JL. Faraday Discuss 2009;141:251-76.
- [126] Berendsen HJC, Grigera JR, Straatsma TP. J Phys Chem 1987;91(24):6269–71.
- [127] Jorgensen WL, Chandrasekhar J, Madura JD, Impey RW, Klein ML. J Chem Phys . 1983;79:926–35.
- [128] García Fernández R, Abascal JL, Vega C, J Chem Phys; 124(14): 144506.
- [129] Abascal JL, Fernández RG, Vega C, Carignano MA. J Chem Phys 2006;125(16): 166101

- [130] Nada H. van der Eerden IPIM. I Chem Phys 2003:118:7401-13.
- [131] Svishchev IM, Kusalik PG, Wang J, Boyd RJ. J Chem Phys 1996;105(11):4742–50.
- Baranyai A, Kiss PT. J Chem Phys 2010;133(14):144109.
- [133] Duh DM, Perera DN, Haymet ADJ. J Chem Phys 1995;102(9):3736–46.
- [134] Vega C, Sanz E, Abascal JLF. J Chem Phys 2005;122(11):114507.
- [135] Jorgensen WL, Jenson C. J Comput Chem 1998;19(10):1179–86.
- [136] Mahoney MW, Jorgensen WL J Chem Phys 2000;112(20):8910–22. [137] Jorgensen WL J Chem Phys 1982;77(8):4156–63.
- [138] Svishchev IM, Kusalik PG. Phys Rev Lett 1994;73(7):975–9.
- [139] Svishchev IM, Kusalik PG. Phys Rev B 1996;53(14):R8815.
- [140] Svishchev IM, Kusalik PG. J Am Chem Soc 1996;118(3):649–54.
- [141] Svishchev IM, Hayward TM. J Chem Phys 1999;111(19):9034–8.
- [142] Drost-Hansen W, Singleton JL, Fundamentals of medical cell biology, chemistry of the living cell., Vol. 3AGreenwich, CT: JAI Press; 1992(Chapter 5).
- [143] Borzsák I, Cummings PT. Phys Rev E 1997;56(6):R6279.
 [144] Borzsák I, Cummings PT. Fluid Phase Equilib 1998;150:141–9.
- [145] Jung DH, Yang JH, Jhon MS. Chem Phys 1999;244(2):331–7
- [146] Watanabe M, Brodsky AM, Reinhardt WP. J Phys Chem 1991;95(12):4593–6.
- [147] Xia X, Berkowitz ML. Phys Rev Lett 1995;74(16):3193.
- [148] Xia X. Perera L. Essmann U. Berkowitz ML. Surf Sci 1995:335:401–15.
- [149] Yan JY, Patey GN. J Phys Chem Lett 2011;2(20):2555-9.
- [150] Yan JY, Patey GN. Chem Eur J 2012;116:7057-64.
- [151] Yan JY, Patey GN. J Chem Phys 2013;139(14):144501.
- [152] Israelachvili JN, McGuiggan PM, Homola AM. Science 1988;240(4849):189.
- [153] Granick S. Science 1991;253(5026):1374.
- [154] Klein J, Kumacheva E. Science 1995;269(5225):816.
- [155] Zhu Y, Granick S. Phys Rev Lett 2001;87(9):096104.
- [156] Raviv U, Laurat P, Klein J. Nature 2001;413(6851):51-4.
- [157] Zangi R, Mark AE. J Chem Phys 2004;120(15):7123-30.
- [158] Fu Z, Luo Y, Ma J, Wei G. J Chem Phys 2011;134(15):154507.
- [159] Nie GX, Wang Y, Huang JP. Front Phys 2015;10(5):106101.
- [160] Qiu H, Guo W. Phys Rev Lett 2013;110(19):195701. [161] Zhang XX, Lü YJ, Chen M. Mol Phys 2013;111(24):3808-14.
- [162] Zhang XX, Chen M, Fu M. Appl Surf Sci 2014;313:771-6.
- 163] Yeh IC, Berkowitz ML. J Electroanal Chem 1998;450(2):313-25.
- [164] Sutmann G. J Electroanal Chem 1998;450(2):289-302.
- [165] Yeh IC, Berkowitz ML. J Chem Phys 1999;110(16):7935-42.
- [166] Vegiri A, Schevkunov SV. J Chem Phys 2001;115(9):4175–85.
- [167] Vegiri A. J Chem Phys 2002;116(20):8786–98.
- [168] Vegiri A. J Mol Liq 2004;112(1):107–16.
- [169] Hu X, Elghobashi-Meinhardt N, Gembris D, Smith JC. J Chem Phys 2011;135(13): 134507
- [170] Hu H, Hou H, Wang B. J Phys Chem C 2012;116(37):19773.
- [171] Khusnutdinoff RM. Colloid J 2013;75(6):726-32.
- [172] Qian Z, Wei G. Chem Eur J 2014;118(39):8922-8
- [173] Zhang XX, Chen M. Acta Phys -Chim Sin 2014;30(7):1208–14.
- [174] Zhu X, Yuan Q, Zhao YP. Nanoscale 2014;6(10):5432-7
- [175] Yan JY, Overduin SD, Patey GN. J Chem Phys 2014;141(7):074501.
- [176] Druchok M, Holovko M. J Mol Liq 2015;212:969-75.
- [177] Mei F, Zhou X, Kou J, Wu F, Wang C, Lu H. J Chem Phys 2015;142(13):134704.
- [178] Glatz B, Sarupria S. J Chem Phys 2016;145(21):211924.
- [179] Grabowska J, Kuffel A, Zielkiewicz J. J Chem Phys 2017;147(17):174502.